Green Chemistry

Accepted Manuscript

ROYAL SOCIETY OF CHEMISTRY

www.rsc.org/greenchem

Journal Name

RSCPublishing

ARTICLE

Transition–metal–functionalized ordered mesoporous silicas: An overview of sustainable chiral catalysts for enantioselective transformations

Cite this: DOI: 10.1039/x0xx00000x

Received 00th January 2012,
Accepted 00th January 2012

DOI: 10.1039/x0xx00000x

www.rsc.org/

Tanyu Cheng, Qiankun Zhao, Dacheng Zhang, Guohua, Liu*

Transition–metal–catalyzed asymmetric reactions have been demonstrated to be powerful methods for enantioselective construction of various optically pure compounds. The development of ordered mesoporous silica-supported chiral transition-metal-based catalysts and the exploration of their applications represent important progress in green chemistry since such an approach enables eco-friendly and sustainable catalytic process. In this review, we focus on recent advances in the preparation of ordered mesoporous silica-supported chiral transition-metal-based catalysts and their applications in enantioselective transformations. Firstly, we provide a brief introduction to the modification of ordered mesoporous silicas. We then present in detail the applications of transition–metal–functionalized ordered mesoporous silicas for enantioselective transformations according to various types of reactions. Lastly, perspectives for the further development of this research area are discussed.

1 Introduction

Catalytic transformations, especially transition–metal catalysis, are important methods for the synthesis of complicated organic compounds, and asymmetric catalysis is one of the most efficient ways to obtain optically pure products.[1-4] These chiral pure compounds, including pharmaceuticals and pesticides, play very important roles in our daily lives. The increasing demand for such compounds continues to promote the development of asymmetric catalytic methodologies and of chiral catalysts. Impressive achievements in this field have been accomplished in the past decades, and the Nobel Prize for Chemistry in 2001 was jointly awarded to W. S. Knowles, R. Noyori, and K. B. Sharpless for their significant contributions in this field.

Although homogeneous asymmetric catalysis has significant benefits involving in high catalytic activity and enantioselectivity, and many remarkable successes have been achieved,[5-10] it also suffers from some intrinsic shortcomings. Normally, transition–metal catalysts is expensive, and is difficult to reuse in homogeneous catalysis system, which is reflected in high costs of the products. In addition, chiral fine chemicals, especially chiral pharmaceuticals, require rigorous purity, thereby general isolation applied in an organic workup procedure is difficult to eliminate all traces of transition–metal catalysts. Furthermore, such procedures also generate copious amounts of waste, making them environmentally unfavorable. Due to these intrinsic shortcomings, development of chiral transition–metal–based heterogeneous catalysts have emerged in a timely fashion as a viable alternative. Generally, heterogeneous catalysts can be easily separated from reaction system through simple operation and reused repeatedly, which greatly decrease the cost of products and the generation of waste. Interestingly, compared with the corresponding homogeneous catalysts, some chiral heterogeneous catalysts have exhibited similar catalytic activities and enantioselectivities, and sometimes are even more selective. This holds great promise for their practical use in the synthesis of valuable optically pure compounds.

With the development of nanomaterial science, many approaches for the preparation of chiral transition–metal–based heterogeneous catalysts have been developed, including the immobilization of various classical transition–metal catalysts on solid materials and the introduction of well–defined single–site catalytically active centres on supports. Among abundant solid supports, silica materials are the most promising solid supports for such applications because of their low price, ready availability, and various morphologies. Since Kresge and co–workers[11] reported an ordered mesoporous silica (MCM–41), a wide scope of mesoporous silica materials with various morphologies have been developed. Recently, some excellent reviews have summarized the procedures for the preparation and functionalization of mesoporous silica materials.[12-15] Generally, mesoporous materials possess several outstanding properties, such as large surface area and pore volume, tunable pore dimensions, well–defined pore arrangement, and high thermal and mechanical stability. These merits make

mesoporous silica materials as excellent supports for construction of various chiral transition–metal–based heterogeneous catalysts. Although some reviews have well–documented in heterogeneous catalysts,[16-20] it is still worthwhile to provide an overview of mesoporous silica–supported chiral transition–metal–based catalysts for enantioselective transformations, as these mesoporous silica–supported chiral transition–metal–based catalysts are on the way from academic research to practical application.

In this review, we provide an overview of enantioselective organic transformations catalyzed by various mesoporous silica–supported chiral transition–metal–based catalysts. In first part, we briefly introduce the modification strategies of mesoporous silicas. Then, the applications of mesoporous silica–supported chiral transition–metal–based catalysts are elaborated according to various types of reactions. Finally, we discuss perspectives for further development in this field.

2 Modifications of mesoporous silicas

Since the first report of a periodic mesoporous silica designated as MCM–41 in the early 1990s,[11] ordered mesoporous silica materials have attracted much attention. Many new synthetic procedures and several kinds of mesoporous silicas have been developed in the past two decades, and some remarkable reviews have summarized relevant documents.[12-15] For the applications of ordered mesoporous silicas as supports to construct silica-supported chiral transition-metal-based catalysts, there are four strategies through the modification and functionalization of ordered mesoporous silicas, namely covalent bonding, adsorption, ion-pair formation, and entrapment (Figure 1).[17]

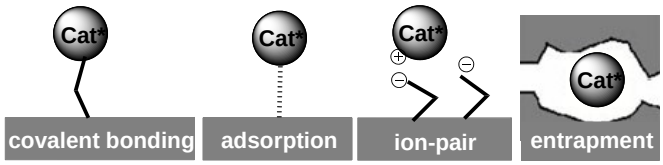

Figure 1 Schematic representation of four immobilization strategies of chiral organometallic complex on mesoporous materials.

Among four immobilization strategies, post-grafting (post-synthesis) and co-condensation (direct-synthesis) are two main methods for construction of mesoporous silica-supported chiral transition-metal-based catalysts (Scheme 1).

2.1 Post-grafting (Post-synthesis)

Post-grafting method refers to the subsequent modification of the surface of ordered mesoporous silicas with functional molecules. This method is used to immobilize mainly an organometallic complex on a support through a covalent bond. The interaction is therefore much more stable than that obtained with physical adsorption. Normally, this procedure is accomplished by reaction between a functional molecule and free silanol group on mesoporous silica surface, as shown in Scheme 1a. There are two main advantages if functional molecule R is a chiral catalyst. First, the structure of mesoporous silica is usually retained as there is no obvious damage during post-grafting process. Second, the chiral microenvironment of supported catalyst is usually maintained because different ordered mesoporous silicas can be screened to find the best fitting support, allowing supported catalysis with desirable enantioselectivity as same as that obtained with its corresponding homogeneous catalyst. However, post-grafting method has also some disadvantages. For example, chiral catalysts grafted within mesoporous channels can decrease pore size, which may reduce catalytic efficiency because of the diffusible block of substrates.

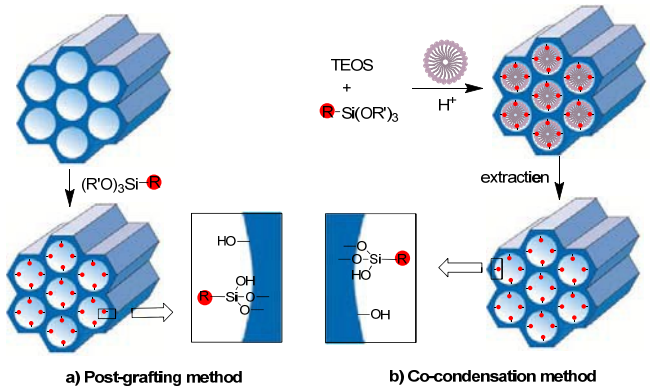

Scheme 1 Schematic representations of the modification of ordered mesoporous silicas by post–grafting and co–condensation methods.

2.2 Co–condensation (Direct–synthesis)

Co–condensation is the most commonly used method for preparing a functional ordered mesoporous silica, especially for a chiral transition–metal–based heterogeneous catalyst. Normally, a typically synthetic procedure involves two steps for the direct synthesis of supported catalysts. Taking co–condensation of tetraethoxysiloxane (TEOS) and chiral organic siloxane $(R'O)_3SiR$ as an example as outlined in Scheme 1b, in the first step, $(R'O)_3SiR$ siloxane with R as a chiral transition–metal–based group is co–condensed with TEOS in the presence of a template under an acidic condition, which can provide an ordered SBA–15–like mesoporous silica. The template is then extracted, leaving a desired chiral transition–metal–functionalized mesoporous material. Compared with post-grafting method, co–condensation has more advantages. The transition–metal–functionalities on a material are distributed evenly on the walls of mesoporous channels. This avoids interference between them, which improves a chance to synthesize multi–functional catalyst through co–condensation of several chiral siloxanes. Also, by this method, suitable pore size and pore arrangement could be obtained, and loaded amount of transition–metal–functionality could be enhanced. However, the disadvantage is that the content of functional parts in an ordered mesoporous silica does not normally exceed 40 mol %, as excess $(R'O)_3SiR$ in a reaction mixture would decrease the orderly degree of mesomaterial. In addition, a

portion of transition–metal–functionalities may be incorporated into pore–wall network, which incurs some loss of functionality.

3 Applications of ordered mesoporous silica–supported transition–metal-based catalysts

3.1 Asymmetric hydrogenation

Asymmetric hydrogenation is a common method for reducing unsaturated compounds with hydrogen, the most prominent advantage is simple workup because of the gaseous reactant. It represents one of the most efficient processes for the synthesis of optically pure molecules. Besides generally physical adsorption or impregnation used in early researches, an ordered mesoporous silica–supported chiral transition–metal-based catalyst could be constructed through two main approaches. One is by a direct grafting or co–condensation of a chiral transition–metal–derived siloxane on a mesoporous material. Another approach is to synthesize a chiral ligand–functionalized material at first, followed by an *in situ* complexation of chiral material and a transition–metal complex. In the following, we describe recent developments concerning the use of chiral transition–metal-based heterogeneous catalysts for asymmetric hydrogenation, mainly focusing on asymmetric hydrogenation of C=C bond and asymmetric hydrogenation of C=O bond.

3.1.1 Asymmetric hydrogenation of C=C bond. Construction of a mesoporous silica–supported chiral transition–metal-based catalyst for asymmetric hydrogenation of C=C bonds was firstly explored by Anderson group.[21] In this early work, they utilized a physical absorption method to impregnate well-known homogeneous chiral phosphine–based complexes within an ordered mesoporous silica of 26 Å (average pore size), constructing two chiral transition–metal-based heterogeneous catalysts. The heterogeneous catalysts were obtained either *via* absorption of Rh–BPPM complex prepared by the reaction of (2*S*,4*S*)-N-(*tert*-butoxycarbonyl)-4-(diphenylphosphino)-2-[(diphenylphosphino)methyl]pyrrolidine) and bis(cycloocta-1,5-diene)dichlorodirhodium ($[Rh(COD)Cl]_2$), or *via* absorption of Ru–BINAP complex (Ru–BINAP = [(*R*)-2,2'-bis(diphenylphosphino)-1,1'-binaphthyl]chloro(*p*-cymene)ruthenium chloride) within this mesoporous silica. As shown in Scheme 2, it was found that both were efficient in the asymmetric hydrogenation of water–soluble sodium salt of *N*-acetamidocinnamic acid (up to 80% *ee*), while gave poor *ee* values for enantioselective transformation of itaconic acid. Similar to the Anderson's report, the Dickson group[22] also immobilized same catalysts on the modified mesoporous silicas by external surface deactivation and/or internal derivatization using the similar impregnation approach. They found that the pore size of the supports greatly affected the catalytic activity and enantioselectivity when sodium *α*–acetamidocinnamate or itaconic acid was reduced in water.

Also, by the use of impregnation approach, Crosman and Hoelderich[23] prepared a series of Al–SBA–15-supported chiral Rh-based heterogeneous catalysts. As shown in Scheme 3, chiral heterogeneous catalysts could be obtained through the impregnation of rhodium diphosphine complexes ([Rh(L-L)COD]Cl: ((L-L) = diphosphine ligand and COD = cyclooctadiene)) within aluminated SBA–15 (Al–SBA–15), where the interaction of the cationic rhodium of organometallic complex with the anionic host framework between Al Lewis acid sites and P Lewis basic sites were responsible for the immobilization of rhodium diphosphine complexes. These heterogeneous catalysts showed high activity and excellent chemo– and enantio–selectivity for the asymmetric hydrogenations of dimethyl itaconate and methyl *α*–acetamidoacrylate up to 93% *ee*, 99% conversion, and 99% selectivity. Furthermore, these catalysts could be reused at least four times without any activity loss, with a TON (turnover number) value larger than 4000. Later, they also utilized Al–MCM-41, Al–MCM-48 as supports[24,25] to construct a series of the same chiral Rh-based heterogeneous catalysts through this impregnation approach. Similarly, these heterogeneous catalysts also showed high activity and excellent chemo– and enantio–selectivity for the asymmetric hydrogenations of dimethyl itaconate and methyl *α*–acetamidoacrylate up to 98% *ee*, 99% conversion, and 99% selectivity. Subsequently, the groups of Sheldon[26] and Hutchings[27] also reported a series of mesoporous silica–supported chiral Rh–diphosphine-based catalysts for asymmetric hydrogenation of C=C bonds.

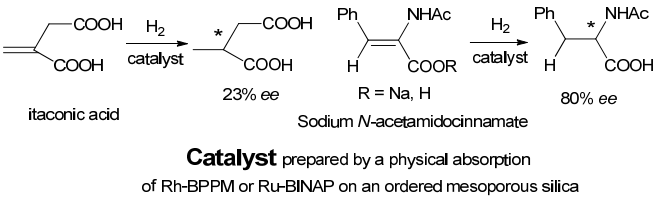

Scheme 2 Asymmetric hydrogenation of itaconic acid and *N*-acetamidocinnamic acid by impregnated heterogeneous catalysts.

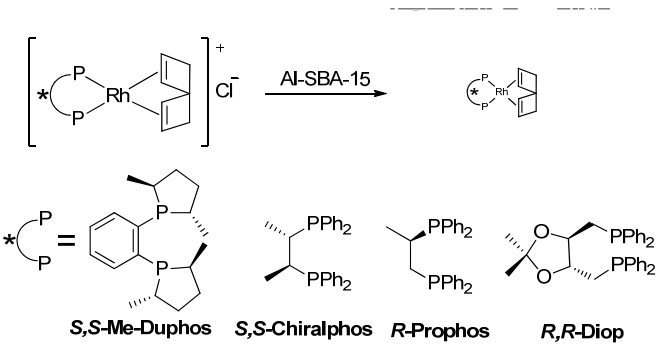

Scheme 3 Structures of the diphosphine ligands and heterogeneous catalysts.

Besides the general application of impregnation approach, Dufaud and co–workers[28] utilized a post-grafting method to prepare chiral Rh-based heterogeneous catalysts by covalent immobilization of DIOP–Rh complex onto SBA–15. As shown in Scheme 4, the homogeneous triethoxysilyl rhodium complex $[Rh(diop)(PPh_2(CH_2)_2Si(OCH_2CH_3)_3)Cl]$ was generated from the reaction of $PPh_2(CH_2)_2Si(OCH_2CH_3)_3$ and $[Rh(COD)Cl]_2$, followed by the substitution of COD ligand by chiral DIOP

ligand. The chiral Rh-based heterogeneous catalyst **1** could then be obtained by directly post-grafting it on SBA-15. Finally, the silica surface of catalyst **1** functionalized by the use of $(CH_3)_3SiCl$ as silylating agent led to catalyst **2**. Both catalysts **1** and **2** exhibited high catalytic activities (up to 84% yield) and moderate enantioselectivities (up to 57% *ee*) for the asymmetric hydrogenation of methyl (*Z*)-2-*N*-acetylaminocinnamate. In addition, the heterogeneous catalyst **1** could be reused four times without obvious loss of its activity and enantioselectivity.

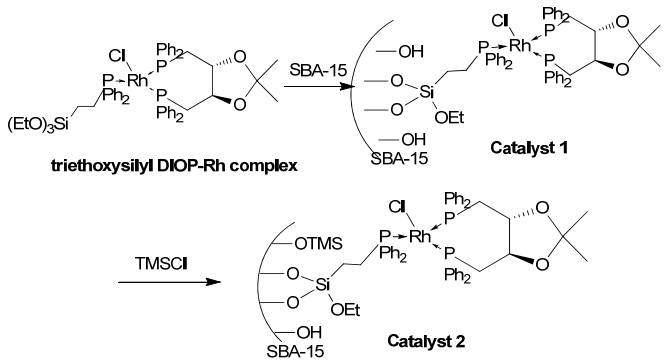

Scheme 4 Preparation of catalysts **1** and **2**.

Similar to direct post-grafting a chiral transition–metal–derived siloxane on a mesoporous material, Sánchez and co–workers[29] also reported several chiral imidazolium–Ru-based complexes onto MCM–41, providing recyclable heterogeneous chiral catalysts (The use of catalyst **3** as a representative as shown in Scheme 5). Catalyst **3** showed excellent catalytic activity (more than 99% yield) and enantioselectivity (98% *ee*) with a TOF (turnover frequency) value of 1400 h^{-1} in the asymmetric hydrogenation of diethyl 2–benzylidenesuccinate, which could also be recycled for five times with less than 1.0% loss of ruthenium after the fifth recycle.

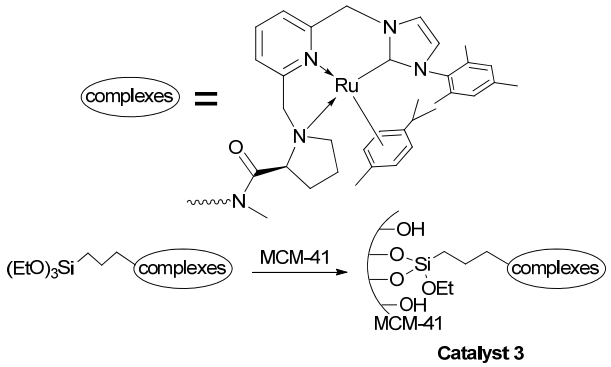

Scheme 5 Preparation of catalyst **3**.

Differed from direct post-grafting a chiral transition–metal–derived siloxane on a mesoporous material, Halligudi group[30] post-grafted a chiral ligand–functionalized material at first followed by an *in situ* complexation, constructing chiral Ir-based heterogeneous catalysts. In the work, they direct post-grafted triethoxysilyl BINOL–derived monodentate phosphorothioite ligand onto various mesoporous silica supports, including SBA–15, MCM–41, and MCM–48, which were coordinated with $[Ir(COD)Cl]_2$ to generate a series of chiral heterogeneous catalysts. Among these catalysts, they found that the iridium complex immobilized on SBA–15 (catalyst **4**) showed the best catalytic performance (up to 94% *ee*, Scheme 6) for the asymmetric hydrogenation of itaconic acid derivatives, which was comparable to that obtained with its homogeneous counterpart (96% *ee*). However, its TON value is only half of its homogeneous counterpart because of the slower interaction between the substrate and the catalyst in heterogeneous system.

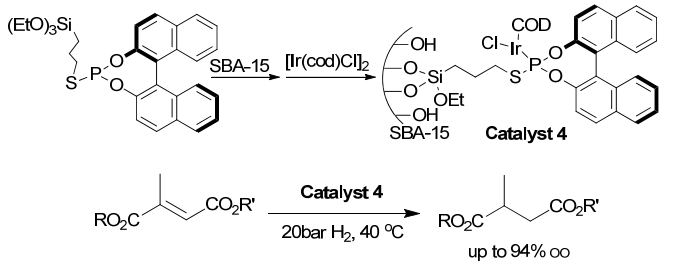

Scheme 6 Structure of catalyst **4** and its application in asymmetric hydrogenation.

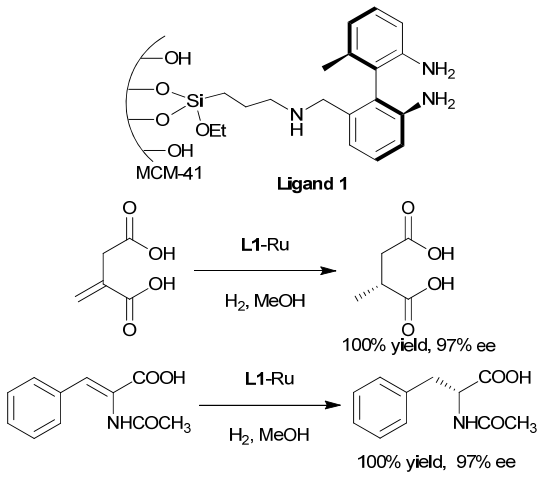

Scheme 7 Structure of ligand **1** and the asymmetric hydrogenation catalyzed by the complex of **L1**–Ru.

In addition of these considerable successes of chiral phosphine–based heterogeneous catalysts, the triethoxysilyl phosphorus–free chiral ligands were also involved to be post-grafted onto mesoporous material. Pérez and co–workers[31] post-grafted a chiral diaminobiphenyl derivative onto MCM–41, providing the supported chiral ligand **1** (Scheme 7). The chiral Ru-based heterogeneous catalyst generated by an *in situ* complexation of ligand **1** and $[Ru(COD)Cl]_2$ exhibited a quantitative yield and 97% *ee* in the asymmetric hydrogenation of *α*,*β*–unsaturated carboxylic acids. More importantly, the enantioselectivity was improved relative to that of less than 80% *ee* of its homogenous counterpart, which was attributed to the increased rigidity of the overall catalytic structure resulting

from the interaction of ligand **1** with the hydroxyl groups on MCM–41.

Interestingly, a more detailed exploration of chiral transition–metal–based heterogeneous catalyst **5** for asymmetric hydrogenation was reported by Raja and co–workers.[32] As shown in Scheme 8, they utilized 3-bromopropyl-functionality onto MCM-41 as a linker to develop a series of chiral Rh-(or Pd)-based heterogeneous catalysts through the reaction with bidentate amines 2-aminomethyl-1-ethyl pyrrolidine (or 1,2-diphenylethylenediamine (DPEN)) followed by the $[Rh(COD)Cl]_2$ (and/or $[Pd(COD)Cl]_2$). The significant benefit was that the BF_4^- anion was hydrogen-bonded to the nitrogen of the amino groups, which could be immobilized steadily rhodium(I) or palladium(II) complexes within the nanopore of MCM-41. As presented in this study, all chiral Rh (or Pd)-based heterogeneous catalysts exhibited efficiently catalytic activity in the asymmetric hydrogenation of *E*-*α*-phenylcinnamic acid and methyl benzoylformate. In particular, the enantioselectivities achieved with catalyst **5** as an example and analogs were far superior to that achieved with their homogeneous counterparts, which ascribed the restricted access generated by the concavity of the pores.

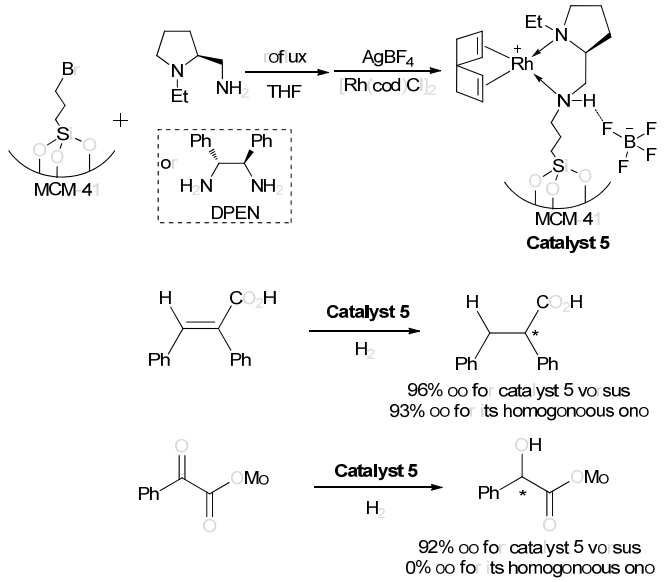

Scheme 8 Structure of catalyst **5** and its application in asymmetric hydrogenation.

3.1.2 Asymmetric hydrogenation of C=O bond. Besides the applications of mesoporous silica–supported chiral transition–metal–based catalysts in the asymmetric reduction of C=C bonds, lots of works had involved in the enantioselective hydrogenation of C=O bonds. An early work was reported by Ghosh and Kumar.[33] As shown in Scheme 9, they utilized the post–grafting method to construct two chiral Ru-based heterogeneous catalysts **6** and **7**. It was found that the highly ordered hexagonal and cubic patterns of MCM–41 and MCM–48 were retained after modification with the Ru complexes. Catalyst **7** showed much higher enantioselectivity than catalyst **6** in the asymmetric hydrogenation of prochiral ketones, indicating that both chiral biphosphine and diamine ligands are necessary to achieve maximum enantioselectivity in the asymmetric hydrogenation. Taking asymmetric hydrogenation of acetophenone as an example, catalyst **7** gave 99% *ee* value while catalyst **6** only afforded 31% *ee*. In addition, the catalysts could be effectively recycled and reused four times without obvious loss of the catalytic performance. Also, Lin group[34] post-grafted successfully triethoxysilyl 4,4'–substituted BINAPs onto SBA–15, constructing a chiral BINAP-based ligand. The chiral Ru-based heterogeneous catalyst generated by an *in situ* complexation with $[RuCl_2(p\text{-cymene})]_2$ was also highly efficient and recyclable in the asymmetric hydrogenation of *β*–aryl *β*–keto esters, which could provide the corresponding chiral products with up to 98.6% *ee*. Later, they also immobilized chiral $RuCl_2$–diphosphine–diamine complexes, containing dual chiral ligands similar to those in Kumar's catalyst, on mesoporous silica nanospheres with three–dimensional channels.[35,36] These catalysts exhibited high catalytic efficiency in the hydrogenation of ketones. Similarly, these catalysts had also been used in the asymmetric hydrogenation of racemic aryl aldehydes with high catalytic efficiency. Meanwhile, the similar other Ru complexes with chiral 1,2-diaminocyclohexane (DACH)[37] and DPEN[38,39] ligands on mesoporous silica materials could be constructed through a post–grafting or ionic bond adsorption methods, where they were efficient in the asymmetric hydrogenation of various ketones.

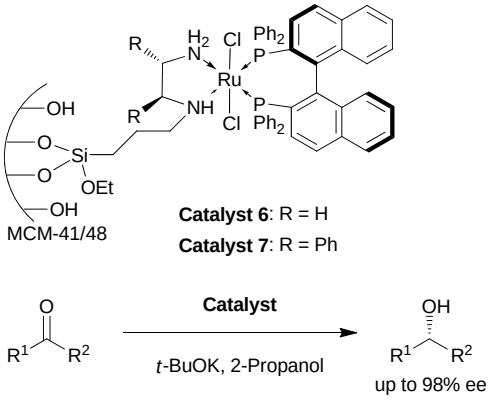

Scheme 9 Structures of catalysts **6** and **7** and their application in the asymmetric hydrogenation of ketones.

It was worth mentioning that periodic mesoporous organosilica (PMO) as a support also enabled to construct various chiral transition–metal–based catalysts. Li group[40] took use the co–condensation method to successfully anchor triethoxysilyl 4,4'–substituted BINAPOs onto silicated framework on PMO, constructing a highly ordered 2D hexagonal structural chiral BINAP-functionalized PMO ligand **2** through an *in situ* reduction as shown in Scheme 10. The chiral Ru-based heterogeneous catalyst generated by an *in situ* complexation with $[RuCl_2(benzene)]_2$ was highly efficient in the asymmetric hydrogenation of *β*–keto esters, which *ee* values were as same as its homogeneous counterpart. Later, Crudden

group[41] also prepared a similar phosphane–containing PMO–supported Ru-based catalyst, which could be also applied to asymmetric transfer hydrogenation of *β*–keto esters with quantitative yield and the same enantioselectivity as its homogeneous counterpart. The studies described here offered a new approach towards the construction of crystal–like rigid chiral walls to induce chirality in asymmetric reactions.

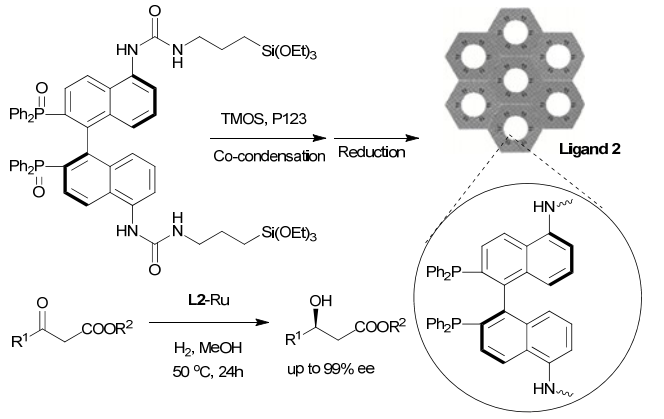

Scheme 10 Preparation of supported Ligand **2** and the asymmetric hydrogenation of *β*–keto esters catalyzed by **L2**–Ru.

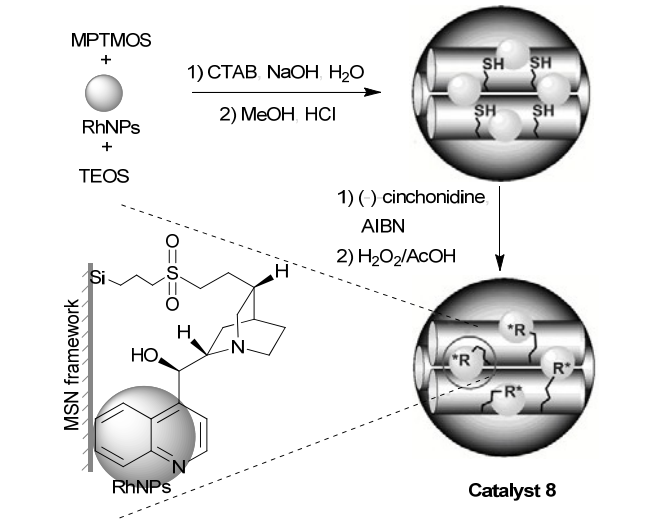

Scheme 11 Preparation of catalyst **8**.

Besides chiral Ru–based heterogeneous catalysts, chiral Rh- and Ir-based heterogeneous catalysts could be also employed in various asymmetric hydrogenation. Lin and co–workers[42] developed a new strategy for the construction of a chiral Rh-based heterogeneous catalyst **8**. As shown in Scheme 11, rhodium nanoparticles (RhNPs) with an approximate diameter of 2.0 nm could be encapsulated uniformly within the framework of an ordered mesoporous silica nanoparticles. The thiol groups were then introduced into the support during the co–condensation of 3-mercaptopropyltrimethoxysiloxane (MPTMOS) and TEOS, which was used as a linker for the anchor of chiral cinchonidine. Finally, coordination with Rh center on the RhNPs formed a chiral catalytic environment, leading to the formation of the heterogeneous catalyst **8**. The catalyst **8** gave the chiral product with 58% *ee* in the asymmetric hydrogenation of ethyl pyruvate. Interestingly, catalyst **8** could be recycled for more than ten times without loss of its enantioselectivity.

Liu and co–workers[43,44] also reported two chiral Ir-based heterogeneous catalysts. As shown in Figure 2, catalyst **9** was prepared by directly postgrafting organometallic complex $IrCl[PPh_2(CH_2)_2Si(OEt)_3]_2[(R,R)$-DPEN] on SBA-15, whereas catalyst **10** was obtained through the co-condensation of TEOS and TsDPEN-siloxane followed by complexation with $[Cp^*IrCl_2]_2$. Both catalysts gave chiral products with up to 99% *ee* in the enantioselective hydrogenation of aromatic ketones. Meanwhile, two SBA–15–supported chiral Rh- and Ru-based catalysts **11** and **12** with dual chiral ligands prepared by a post–grafting method did also exhibited the same catalytic activities and enantioselectivities as its homogeneous counterpart in the asymmetric hydrogenation of aromatic ketones.[45]

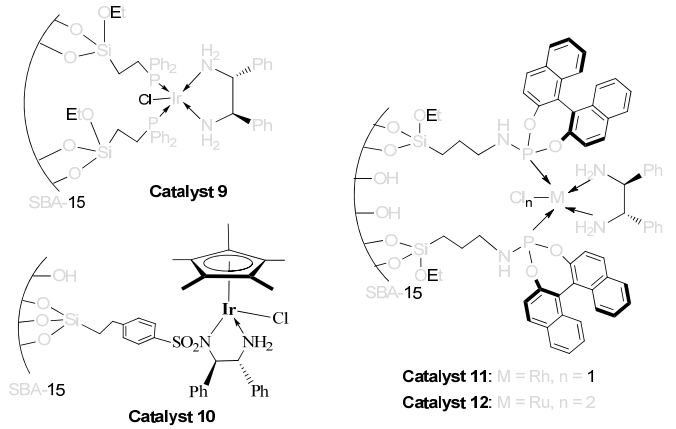

Figure 2 Structures of catalysts **9**–**12**.

3.2 Asymmetric transfer hydrogenation (ATH).

Although some successful examples of asymmetric hydrogenation have been achieved, high pressure of hydrogen and requirement of special equipment still limit its practical application. Recently, asymmetric transfer hydrogenation (ATH) has attracted a great deal of interest because of its mild reaction condition, simple operation, and high yield and enantioselectivity. In addition, many ATH reactions can be carried out in water, which is eco–friendly. In this part, more examples had been performed successfully in ATH reactions through the use of various mesoporous silica–supported chiral transition–metal catalyst.

3.2.1 Chiral Ru–based heterogeneous catalysts. TsDPEN–derived siloxane as an efficient chiral siloxane could be used extensively to construct various transition–metal–based heterogeneous catalysts for asymmetric transfer hydrogenation. An earlier work was reported by Tu group.[46-48] In their study, they successfully grafted TsDPEN–derived siloxane on amorphous silica gel, mesoporous MCM–41, and SBA–15. The *in situ* complexation them with $[RuCl_2(p$-cymene$)_2$ then led to three corresponding chiral Ru–based heterogeneous catalysts.

Generally, three heterogeneous catalysts enabled ATH reactions both in organic solvent and water. Although the mesoporous silica–supported heterogeneous catalysts displayed worse recyclability than that of the corresponding amorphous silica gel–supported one, this work motivated a further exploration on the use of various mesoporous silica–supported chiral transition–metal catalyst for ATH reaction.

Similar to the Tu's work, Ying group[49] also synthesized a chiral Ru–based heterogeneous catalyst by the same post–grafting method. Difference was that they used siliceous mesocellular foam (MCF) as a support to construct a MCF–supported chiral Ru–based heterogeneous catalyst, in which the catalyst was generated by the *in situ* complexation of TsDPEN–derived siloxane onto MCF with $[RuCl_2(p\text{-cymene})_2]$. Unlike the result of Tu's work, the MCF–supported chiral Ru-based heterogeneous catalyst displayed excellent reactivity and high enantioselectivity in the ATH reactions of both imines (up to 90% *ee*) and ketones (up to 97% *ee*) using HCOOH–Et_3N as the hydrogen source. More interestingly, this catalyst had an enhanced reusability in the ATH of 6,7-dimethoxy-1-methyl-3,4-dihydroisoquinoline.

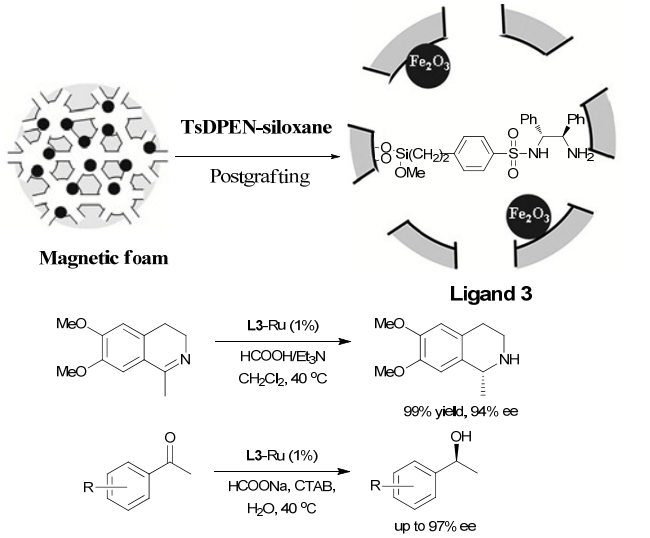

Scheme 12 Preparation of supported Ligand **3** and the ATH catalyzed by **L3**–Ru.

Recently, Li and co–workers[50] further developed MCF–supported method. In this case, they utilized magnetic MCF as a support to construct a magnetic MCF–supported chiral ligand **3**. As shown in Scheme 12, the magnetic heterogeneous catalyst could be generated by the *in situ* complexation of ligand **3** and $[RuCl_2(p\text{-cymene})]_2$. The notable benefit of this magnetic catalyst did not only display high catalytic efficiency in the ATH of various imines and aromatic ketones, but also had a high recyclability in the ATH of 6,7-dimethoxy-1-methyl-3,4-dihydroisoquinoline that could reused repeatedly at least nine times without loss in its enantioselectivity.

An improved immobilization method was further explored by their group[51]. In this case, they utilized mesoporous SBA–16 as a support and impregnated a homogeneous chiral Ru–TsDPEN complex [TsDPEN–RuCl–(cymene)] within its nanocage, developing a SBA–16–supported chiral Ru–based heterogeneous catalyst **13**, as shown in Scheme 13. The benefit of this catalyst was similar to a nanoreactor, in which the tailored pore entrance of SBA–16 effectively confined the homogeneous Ru–TsDPEN catalyst within the mesoporous cage while the suitable pore size allowed substrates and products to freely diffuse. As presented in their study, catalyst **13** did not only exhibit comparable enantioselectivity to its homogeneous counterpart, but also could be recovered and reused without significant loss in catalytic performance. Besides the complexation of TsDPEN–derived siloxane and $[RuCl_2(p\text{-cymene})]_2$, the complexation of it and $[RuCl_2(C_6Me_6)]_2$ also construct a three–dimensional chrysanthemum–like chiral Ru–based heterogeneous catalyst.[52] The heterogeneous catalyst enabled aqueous ATH transformation with an extensive range of substrates including various ketones and quinolines, offering chiral products with excellent catalytic activity (up to 99% *ee*), enantioselectivity (up to 98% *ee*), and a high recyclability (ten times recycle) in the ATH of acetophenone.

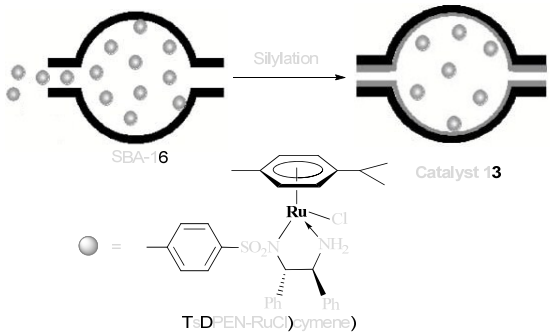

Scheme 13 Preparation of catalyst **13**.

Furthermore, the use of chiral Ru–based heterogeneous catalyst could also be extended to a multiple–step cascade organic transformation. Very recently, Liu group[53] utilized the combined imidazolium–supported organopalladium–functionalized catalyst **14** and chiral Ru–based heterogeneous catalyst **15** (Scheme 14) to realize the Suzuki–ATH cascade reaction to synthesis of biaryl alcohols from haloacetophenones and arylboronic acids in a two–step, one–pot process. The significant benefit of this cascade reaction not only overcame the intrinsic incompatibility of two distinct organometallic complexes, but also realized the enantio–relay catalysis. In particular, this strategy is attractive in the practical organic transformations for construction of a variety of chiral biaryl alcohols. Also, both heterogeneous catalysts could be recycled without loss of its catalytic activity.

More interestingly, apart from the enantio–relay catalysis of two–step one–pot process, the use of a bimetallic Ru/Pd–based heterogeneous catalyst could also realize an enantio–relay catalysis in a one–step one–pot process. As shown in Scheme 15, the bimetallic Ru/Pd–based heterogeneous catalyst **16** could be constructed through the co–condensation of chiral TsDPEN–derived siloxane,

bis[(diphenylphosphino)ethyltriethoxysiloxane)]palladium dichloride and 1,2-bis(triethoxysilyl)ethylene followed by complexation with $(AreneRuCl_2)_2$.[54] Differed from the proceeding of enantio–relay catalysis in two–step one–pot process catalyzed by catalysts **14** and **15**, this one–pot cascade reaction occured the Ru–catalyzed ATH reaction at first, then the Pd–relay–catalyzed cross–coupling of haloacetophenones and arylboronic acids proceeded. The main advantage of catalyst **16** possessed a site–isolated organoruthenium–/organopalladium active species within its PMO network, which could be used to prepare various chiral biaryl alcohols from haloacetophenones and arylboronic acids, with quantitative conversions and up to 98% enantioselectivity in an aqueous medium. This characteristic offered a new approach to realize a highly efficient one–pot cascade reaction with a high recyclability.

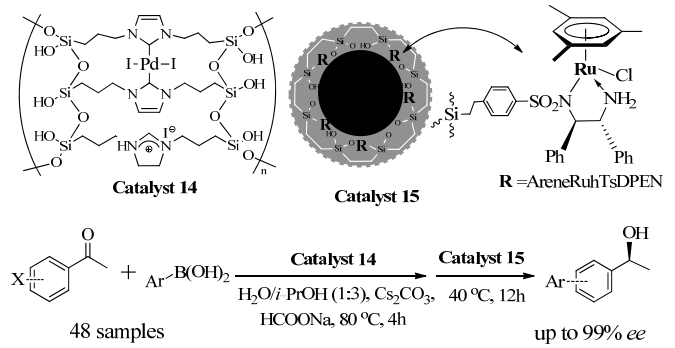

Scheme 14 Structures of catalyst **14** and **15** and their application for the synthesis of biaryl alcohols.

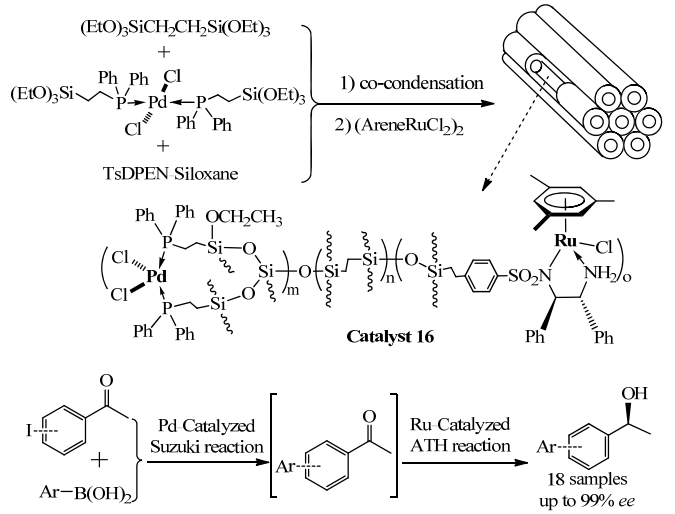

Scheme 15 Preparation of catalyst **16** and its catalytic application in the one–pot cascade reaction.

In addition to the general use of TsDPEN–derived siloxane, chiral 2-aminoethanol is also a suitable ligand to construct chiral Ru–based heterogeneous catalyst for ATH reaction. Jin group[55] prepared a SBA–15–supported chiral norephedrine–based ligand **4** through a post–synthesis method (Figure 3), in which the heterogeneous catalyst could be generated by an *in situ* complexation with $[Ru(hexamethylbenzene)Cl_2]_2$. This heterogeneous catalyst was efficient in the ATH, which had comparable enantioselectivity to its homogeneous chiral ephedrine. Similarly, the Singh group[56] also constructed two SBA–15–supported chiral Ru–based heterogeneous catalysts **17** and **18** (Figure 3) through the same post–synthesis method. It was found that both catalysts are efficient in the ATH of aromatic ketones with 14% to 60% yields and 44% to 93% *ee*.

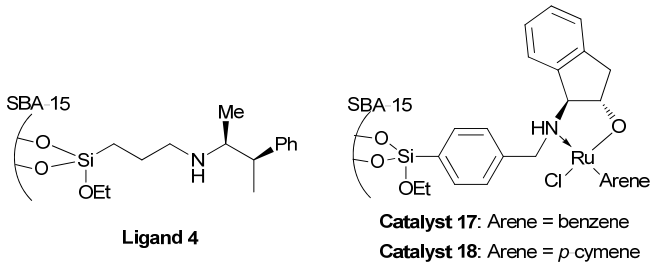

Figure 3 Structures of supported ligand **4** and catalysts **17** and **18**.

3.2.2 Chiral Rh–based heterogeneous catalysts. Besides ruthenium, rhodium is also an important element to prepare efficient chiral Rh–based heterogeneous catalysts for asymmetric transfer hydrogenation.

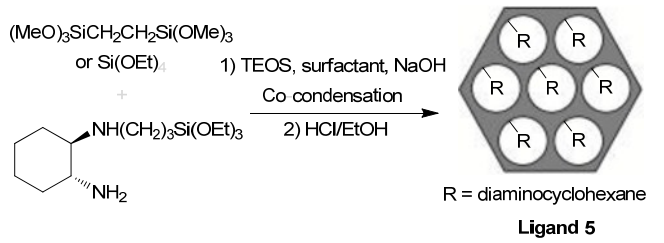

Scheme 16 Preparation of supported ligand **5**.

Earlier report was developed by the Li and co–workers.[57] In their work, they described the co–condensation of chiral *N*-[(triethoxysilyl)-propyl]cyclohexyldiamine-derived siloxane and 1,2-bis(trimethoxysilyl)ethane using octadecyltrimethylammonium chloride as a template under basic conditions, preparing a dimensional–hexagonal structural chiral cyclohexyldiamine–based PMO-supported ligand **5** (Scheme 16). The chiral Rh–based heterogeneous catalyst generated by the *in situ* complexation of ligand **5** and $[Rh(cod)Cl]_2$ was efficient in the ATH of acetophenone although enantioselectivity was poor. Later, they also constructed another large–pore chiral cyclohexyldiamine–based PMO[58] using a triblock copolymer P123 as template under an acidic condition. This heterogeneous catalyst generated by an *in situ* complexation with $[Rh(cod)Cl]_2$ displayed a slightly improved enantioselectivity relative to above catalyst in the ATH of acetophenone. Furthermore, in this case, eight aromatic ketones were converted smoothly to the corresponding chiral alcohols with 18% to 74% *ee*. However, due to the *in situ* complexation method, high leaching (23% leaching of rhodium

after the first reaction) of rhodium are responsible for its low recyclability.

Further endeavor to construct chiral Rh–based heterogeneous catalysts was also attempted by their group.[59] In this work, they utilized benzyl– or propyl–bridged group as a linker to develop two Rh–based heterogeneous catalysts through an improved co–condensation method followed by the similar complexation with $[Rh(cod)Cl]_2$. In this case of co–condensation method, they added 1,3,5-trimethylbenzene (TMB) to the system during the co–condensation under basic conditions.[60] As a result, it was found that the addition of TMB could not only expand the pore diameter, but also induced the structural transformation from the ordered 2D–hexagonal mesostructure to the MCF–like mesostructure, or to the mixture of vesicle and worm–like structure. More importantly, the MCF–like–supported catalyst could enhance greatly catalytic activity in the ATH reaction. Similarly, co–condensation or self-assembly of chiral *N*-[(triethoxysilyl)-propyl]cyclohexyldiamine-derived siloxane and tetraethoxysiloxane (TEOS) also constructs differently morphological chiral Rh–based heterogeneous catalyst. These morphologies include SBA-15-type mesoporous silica, core–shell structured and flower-like nanoparticules, which had been applied to various ATH reactions.[61-63]

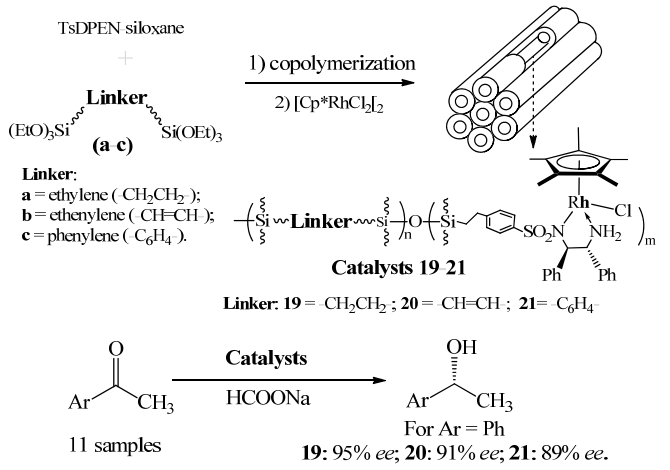

Scheme 17 Preparation of catalyst **19–21** and their catalytic application.

A systemic investigation of the role of organosilica–bridged linker was further enriched by Liu group.[64] As shown in Scheme 17, taking use of TsDPEN–derived siloxane as a chiral siloxane, three typical types of organosilica–bridged PMOs (ethylene–bridged, ethenylene–bridged and phenylene–bridged) were obtained using a co–condensation method. Three Rh–based heterogeneous catalysts **19–21** generated by the *in situ* complexation with $(Cp^*RhCl_2)_2$ had the similar dimensional–hexagonal mesostructures, in which obvious differently enantioselective performances in the ATH of aromatic ketones could be observed. It was found that organosilica–bridged linker played an important role in the enantioselective performance, which the ethylene–bridged catalyst could retain the homogeneous enantioselective performance while ethenylene–bridged or phenylene–bridged catalysts had a worse enantioselectivity due to the additional π–π interactions between the unsaturated bond in the bridging units and phenyl moiety of the chiral ligand within nanochannels. Interestingly, the additional π–π interactions might disappear when phenylene–bridged linker was on the outside surface of mesoporous material. In this case, Liu group[65] reported phenylene–bridged coated magnetic nanoparticles through the co–condensation of chiral TsDPEN–derived siloxane and phenylene–bridged siloxane, in which phenylene–bridged coating is on the outside surface of magnetic nanosphere. The result showed that the heterogeneous catalyst displayed comparable enantioselective performance to its homogeneous counterpart. More importantly, the benefit of this magnetic catalyst not only promoted the catalytic performance because of the hydrophobic nature of phenylene–coated layer, but also allowed highly efficient recovery using an external magnet due to the merits of magnetic material.

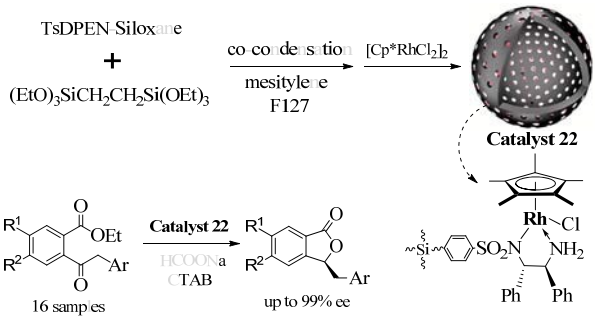

Scheme 18 Preparation of catalyst **22** and its catalytic application.

Besides the general application of organosilica–bridged PMO for the singe–step ATH reaction, chiral Rh–based heterogeneous catalyst could also be extended to enantioselective tandem reaction. Recently, Liu and co–workers[66] reported a hollow–shell structured chiral Rh–based heterogeneous catalyst **22**, as shown in Scheme 18. In this work, the co–condensation 1,2-bis(triethoxysilyl)ethane and chiral TsDPEN–derived siloxane using pluronic F127 as a surfactant and mesitylene as a micelle swelling agent could provide a hollow–shell structured PMO material, which was coordinated with $(Cp^*RhCl_2)_2$ to generate catalyst **22** with about 20 nm of uniformly dispersed hollow–shell structured nanospheres. As demonstrated in the study, catalyst **22** displayed excellent catalytic activity and high enantioselectivity in the tandem reduction-lactonization of ethyl 2-acylarylcarboxylates, where the ATH of ethyl 2-acylarylcarboxylates occurs at first followed by lactonization reaction proceeds to synthesize various chiral phthalides. It is worth mentioning that the catalyst showed higher initial activity than its homogeneous counterpart. That may due to the high hydrophobicity of the hollow-shell-structural nanospheres. In addition, catalyst could be also recycled ten times without significant loss of reactivity.

An interesting work is to use SBA–16 as a support to construct a chiral Rh–based heterogeneous catalyst **23**[67] (Scheme 19). In this work, catalyst **23** could be obtained

through the use of a surface–bound triflate ($CF_3SO_3^-$) counterion to entrap the cationic catalyst $(Cp^*RhTsDPEN)^+(CF_3SO_3)^-$ within methylsilylated SBA–16. It was found that catalyst **23** presented a highly catalytic efficiency in the ultrasound–promoted ATH of aromatic ketones, which enantioselectivity was comparable to its homogenous counterpart. Notably, the ultrasound as nontraditional, high efficient methodology could enhance significantly the reaction rate from hours to minutes. Furthermore, the heterogeneous catalyst could be recovered easily and reused repeatedly nine times without an obvious effect on its enantioselectivity. Similarly, by utilizing an organic–inorganic hybrid silica as a support, it could also construct a chiral Rh–based heterogeneous catalyst **24**.[68] As shown in Scheme 19, the direct postgrafting of chiral TsDPEN–derived siloxane onto an imidazolium–based organic–inorganic hybrid silica followed by the complexation with $(Cp^*RhCl_2)_2$ leads to a high efficient heterogeneous catalyst **24**, in which an imidazolium–functionality in catalyst **24** could substitute Bu_4NBr to function as a phase-transfer role to boost the catalytic performance in the ATH reactions of various aromatic methyl ketones, cyclic and acyclic ketones in aqueous medium.

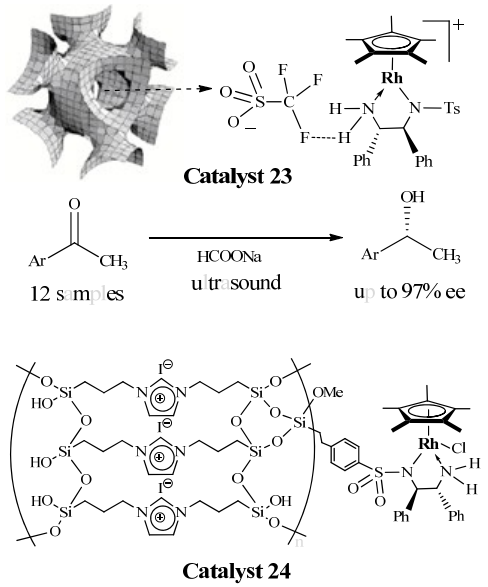

Scheme 19 Preparation of catalyst **23** and its catalytic application and structure of catalyst **24**.

3.2.3 Chiral Ir–based heterogeneous catalysts. Among chiral transition–metal–based heterogeneous catalysts, a few examples were involved in the use of chiral Ir–based heterogeneous catalysts for asymmetric transfer hydrogenation. In an earlier work, Liu group[69] reported a SBA–15–supported chiral Ir–based heterogeneous catalysts through a post–grafting method. As shown Scheme 20, in this work, chiral quinine–based ligand **6** could be obtained using a thiol–ene click reaction of mercapto–functionalized SBA–15 and 9-amino epi-cinchonine. The heterogeneous catalyst generated by an *in situ* complexation with $[Ir(cod)Cl]_2$ displayed efficient catalytic activity in the ATH of aromatic ketones. Interestingly, the heterogeneous catalyst had an enhanced enantioselectivity relative to its homogeneous counterpart (heterogeneous 66% *ee* versus homogeneous 60% *ee*), which may be attributed to the confinement effect. Furthermore, this catalyst could be regenerated with very tiny loss after fourth run.

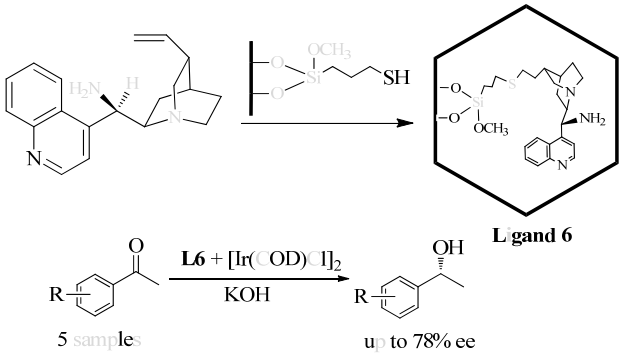

Scheme 20 Preparation of supported ligand **6** and the ATH of aromatic ketones catalyzed by **L6**–Ir.

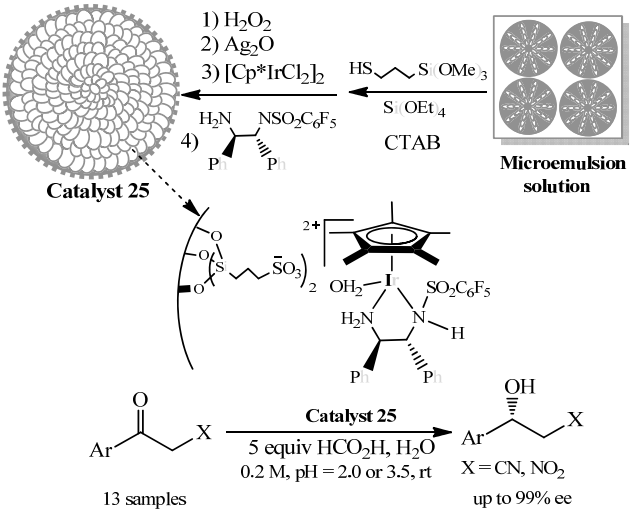

Scheme 21 Preparation of catalyst **25** and its catalytic application.

Another example was developed by Liu group.[70] In this work, by taking use of a chrysanthemum–like mercapto–functionalized mesoporous silica as a support, chiral Ir–based heterogeneous catalyst **25** could be obtained through continuous ion exchange with Ag_2O and $(Cp^*IrCl_2)_2$, followed by complexation of chiral pentafluorophenylsulfonyl-1,2-diphenylethylenediamine, as shown in Scheme 21. Interestingly, in the ATH of various α–cyano and α–cyanoacetophenones under an acidic condition, catalyst **25** displayed a higher catalytic activity and enantioselectivity than its homogeneous counterpart. Also, it could be could be recovered conveniently and subsequently reused without affecting its catalytic activity. More recently, using the similar immobilization method, two more efficiently chiral Ir–based heterogeneous catalysts were also reported.[71,72] Differed from the catalyst **25**, the hydrophobic nature of both catalysts and the well–defined

uniformly distributed active iridium species greatly enhanced the catalytic performance in the ATH of both *α*–cyano and *α*–cyanoacetophenones, even in the ATH of *β*–keto esters.

3.3 Asymmetric oxidation

Oxidation, especially asymmetric oxidation, is a kind of common and important organic reactions. Nowadays, asymmetric oxidation have attracting much interest for the synthesis of valuable molecules. For example, chiral oxirane products are active and significant intermediates for several biologically active compounds. In addition, asymmetric epoxidation of alkenes is the most interesting area because it can provide two chiral centres in one reaction process. In this case, mesoporous silica–supported chiral transition–metal-based catalysts are mainly used in asymmetric epoxidation, asymmetric dihydroxylation, asymmetric oxidation of sulfide to sulfoxide, and asymmetric oxidative kinetic resolution.

3.3.1. Asymmetric epoxidation. In earlier work, Hutchings group[73-75] prepared a chiral Mn–based heterogeneous catalyst by modifying the support of manganese–exchanged Al–MCM–41 to impregnate a chiral salen ligand, *N*,*N*-bis(3,5-di-*tert*-butylsalicylidene)cyclohexane-1,2-diamine within Al–MCM–41 (Scheme 22). The catalyst generated by the reaction of the absorbed Mn-MCM-41 and salen ligand could be used to the enantioselective epoxidation of stilbene when iodosylbenzene was chosen as an oxygen donor. It was found that both reaction temperature and solvent greatly affected the enantioselectivity. Under the optimal conditions, the catalyst provided corresponding epoxide products with 70% yield and 70% *ee*, which is slightly less than its homogeneous counterpart.

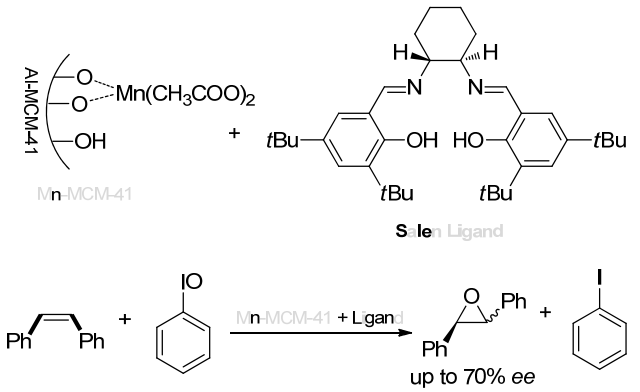

Scheme 22 Structure of salen ligand and the epoxidation catalyzed by the complex of Mn-MCM-41 and salen ligand.

Later, Li group[76] utilized a post-grafting method to prepare a series of chiral Mn-based heterogeneous catalysts **26** (Scheme 23) by directly immobilizing chiral Mn(salen) complexes on mesoporous silica materials through a phenylsulfonic group. In their work, the supports modified with phenyl group were sulfonated with 10% fuming sulfuric acid. After converting the phenylsulfonic groups into sodium sulfonate, heterogeneous catalysts were obtained by anchoring chiral Mn(salen) complexes on the supports by an ion–exchange procedure. These resulting catalysts displayed much higher enantioselectivities than the corresponding homogeneous catalyst in the epoxidation of *α*-methylstyrene and *cis*-*β*-methylstyrene using NaOCl as an oxygen donor in CH_2Cl_2. However, lower yields were obtained compared to those obtained from the homogeneous system. The authors attributed the increase in *ee* values to specific effects, including a surface effect originating from the support as well as the immobilization mode, while the decrease in yield was mainly due to the limited diffusion under the heterogeneous conditions. Another disadvantage of this catalytic system is that the oxidant and solvent (NaOCl as an oxidant and CH_2Cl_2 as a solvent) are not eco-friendly, which is the common problem for the oxidation reaction. Also, they immobilized Mn(salen) complexes on mesoporous materials through phenoxy groups according to a similar procedure.[77] These chiral heterogeneous catalysts showed comparable enantioselectivities in the asymmetric epoxidation of styrene and 6-cyano-2,2-dimethylchromene, and had much higher enantioselectivity for epoxidations of *α*-methylstyrene (heterogeneous 79.7% *ee* versus homogeneous 26.4% *ee*) and *cis*-*β*-methylstyrene (heterogeneous 94.9% *ee* versus homogeneous 25.3% *ee* for *cis*-epoxide) than the homogeneous catalysts. Similarly, Li and co–workers[78,79] also anchored Mn(salen) complexes in nanopores or on the external surface of mesoporous material through phenylsulfonic groups with different linker lengths. The results showed that, for the catalysts immobilized in nanopores, the enantioselectivities were enhanced with increasing linker length, whereas the *ee* values were almost unchanged for the catalysts anchored on the external surface. Moreover, the modification of nanopore surface by methyl groups enabled to improve the catalytic performance for the epoxidation reaction. In addition, a detail investigation of asymmetric epoxidation of 6-cyano-2,2-dimethylchromene was further explored.[79]

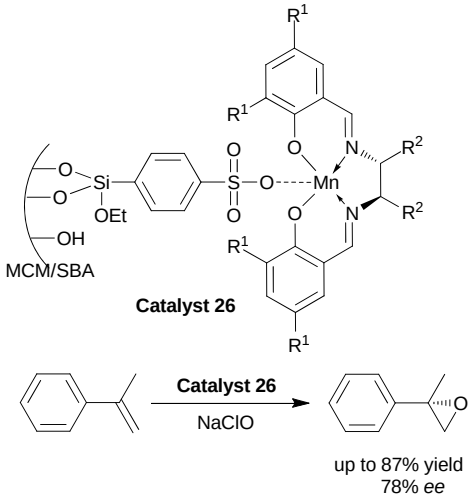

Scheme 23 Structure of catalyst **26** and its catalytic application.

Similar to Li's anchoring method of ion–exchange, Freire group[80] immobilized a derivative of Jacobsen's catalyst through axial coordination of the metal centre on mesoporous silicas, as

shown in Figure 4. In their research, the supports were first modified with 3-aminopropyltriethoxysiloxane (APTES). The Mn(salen) complex was then directly anchored on the amino–functionalized material through a coordinative bond. The obtained catalyst **27** gave the corresponding chiral products with up to 97% conversions and up to 64% *ee* for the asymmetric epoxidation of styrene, *α*-methylstyrene, and 6-cyano-chromene using *m*-CPBA/NMO (*m*-CPBA = *m*-chloroperoxybenzoic acid; NMO = 4-methylmorpholine *N*-oxide) as the oxidant. The reutilization of the heterogeneous catalyst in less than three recycle leads a gradual decrease of epoxide enantioselectivity and selectivity, indicating deactivation or leaching of Mn(salen) complex by oxidative degradation. Later, Liu and co–workers[81] synthesized a similar MCM–41–type mesoporous silica–supported chiral Mn(salen) catalyst through a co–condensation method. The catalyst also displayed high catalytic activity with up to 90% *ee* in the asymmetric epoxidation of alkenes using *m*-CPBA/NMO as the oxidant.

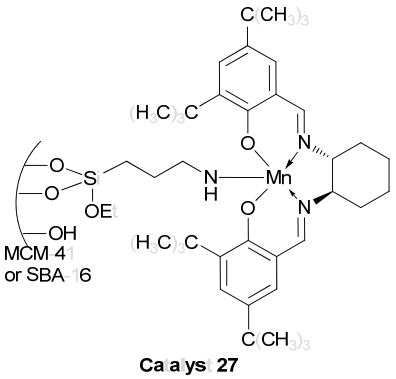

Catalyst 27

Figure 4 Structure of catalyst **27**.

Compared with the methods of ion-pair or coordination bond, a covalent bond method to immobilize a homogeneous catalyst is much more stable. Therefore, immobilization of homogeneous catalysts on mesoporous materials through a covalent bond method is becoming ever more popular. An early work was reported by Kim and Shin.[82] In their work, chiral Mn(salen) complexes were heterogenized on mesoporous silica MCM–41 by a grafting method involving a C=N bond. The prepared heterogeneous Mn(salen)-based catalyst was stable during the oxidation, which exhibited relatively high enantioselectivity in the epoxidation of styrene (heterogeneous 86% *ee* versus homogeneous 65% *ee*) and *α*–methylstyrene (heterogeneous 56% *ee* versus homogeneous 43% *ee*) using NMO as the oxidant. Similarly, by using the same C=N bond, Liu group[83] anchored a chiral Mn(salen) complex onto mesoporous molecular sieves MCM–48 to afford the catalyst **28** (Figure 5). The catalyst **28** gave the chiral products with up to 99% ee value in the asymmetric epoxidation of some aromatic olefins. Interestingly, for asymmetric epoxidation of α-methylstyrene, the ee value was notably increased from 44% (homogeneous catalyst) to more than 99% (heterogeneous catalyst) although the activity was obviously decreased. The enhanced enantioselectivity was attributed to the topological structure of MCM-48 that restrains the free rotation of the intermediate and to the slow diffusion of the reactant and the oxidant into the catalyst. In addition, the recycling experiments showed that the enantioselectivity remained unchanged and the conversion of *α*-methylstyrene decreased slightly after three runs in the epoxidation of *α*-methylstyrene. ICP analysis also indicated that only about 1% Mn leached after the first run.

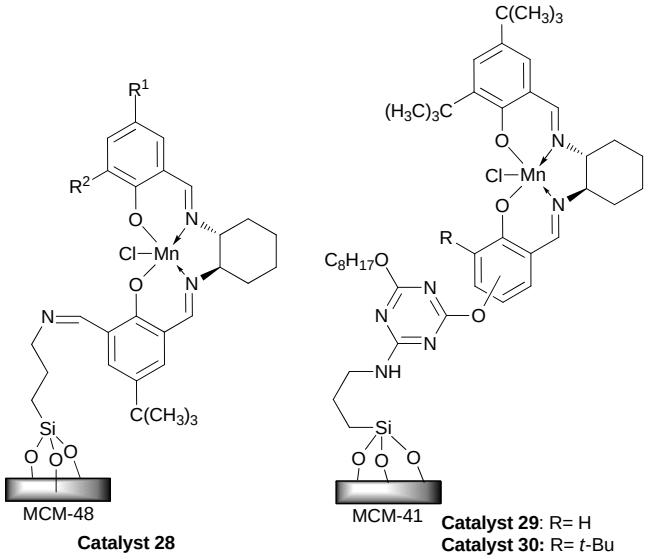

Catalyst 28

Catalyst 29: R= H
Catalyst 30: R= *t*-Bu

Figure 5 Structures of catalysts **28–30**.

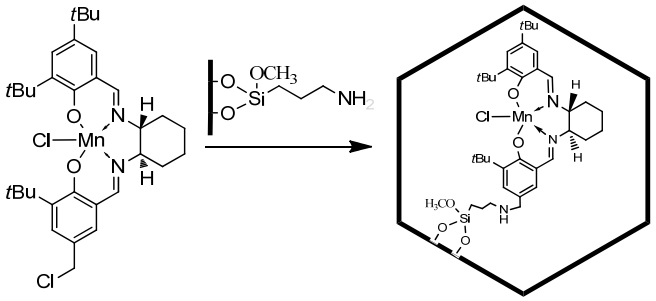

Catalyst 31

Scheme 24 Preparation of catalyst **31**.

Also, another two Mn(salen) complexes were post–grafted onto mesoporous MCM–41, providing Mn-based chiral heterogeneous catalysts **29** and **30** (Figure 5).[84] For the epoxidation of 1-phenylcyclohex-1-ene with *m*-CPBA/NMO as the oxidant, catalyst **30** showed much higher enantioselectivity than catalyst **29** (82% *ee* for **33** versus 34% *ee* for **32**). Notably, the lack of a *tert*-butyl group at the 3–position in catalyst **29** was responsible for its lower *ee* value. At the same time, Kim and co–workers[85] anchored an Mn(salen) complex on organosiloxane–functionalized mesoporous silicas by a post–modification method using a thiol-ene click reaction. Almost the same results were observed for the asymmetric epoxidation of alkenes using *m*-CPBA/NMO as the oxidant as when a was used, in which same enantioselectivities as homogeneous

counterpart could be obtained by the using of heterogeneous catalyst.

Similarly, Kureshy and co–workers[86,87] anchored an Mn(salen) complex onto amino–functionalized mesoporous silicas, MCM–41 and SBA–15 by a post–modification method providing a Mn-based chiral heterogeneous catalyst **31**, as shown in Scheme 24. The supported catalysts showed higher enantioselectivities in the asymmetric epoxidation of non–functionalized alkenes in the presence of pyridine *N*-oxide as an axial base using aqueous NaOCl as an oxidant compared to the reaction catalyzed by the homogeneous Mn complex (heterogeneous 71% *ee* versus homogeneous 48% *ee*). It was also found that the SBA–15–based catalyst displayed higher catalytic efficiency in epoxidation than the MCM–41–based catalyst, which was attributed to the larger pore diameter of the former. Later, several other supported Mn(salen) catalysts[88-93] were also prepared through similar procedures as that reported by Kureshy group. All of them were stable and some of them showed high recyclability.

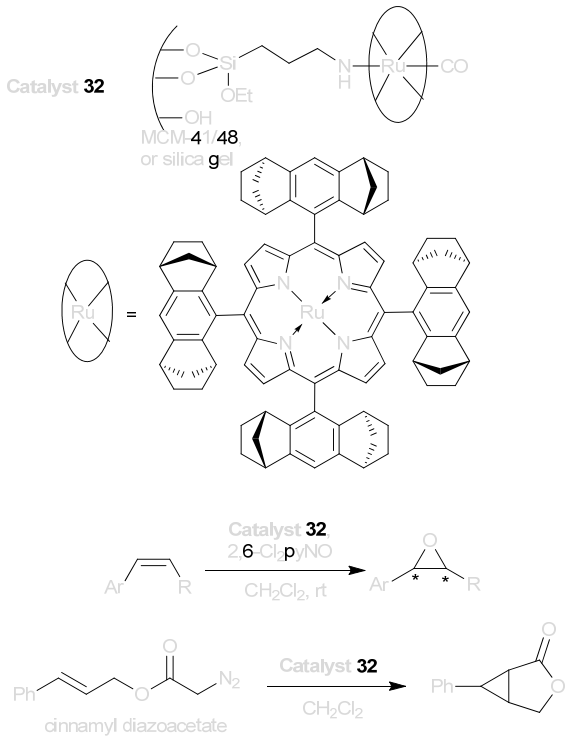

Scheme 25 Structure of catalyst **32** and its catalytic applications.

Besides Mn(salen) complexes, the D_4–symmetric ruthenium complex of [5,10,15,20-tetrakis-(1*S*,4*R*,5*R*,8*S*)-1,2,3,4,5,6,7,8-octahydro-1,2:5,8-dimethano-anthracen-9-yl] porphyrin is an efficient catalyst for asymmetric alkene epoxidation and cyclopropanation. Che and co–workers[94] anchored this chiral complex onto mesoporous MCM-series or silica gel through coordinative bonds to afford catalysts (the use of MCM–48–based **32** as a representative). As shown in Scheme 25, catalysts was used for the asymmetric epoxidation of styrene with 2,6-dichloropyridine N-oxide (2,6-Cl_2pyNO) as an oxidant. It was found that the MCM–48–based catalyst **32** gave the highest *ee* value and yield, while the ruthenium complex anchored on the silica gel leached easily from the surface after the reaction. In order to prove the position of the ruthenium porphyrin in the channels of the mesoporous silicas, a large molecule, cholesterol acetate, was investigated. In this case, it was found that the catalysts supported on MCM–41 and MCM–48 could not catalyze the epoxidation, whereas the homogeneous Ru complex gave the epoxide product in high yield and selectivity, confirming that the ruthenium porphyrin was encapsulated in the channels of the mesoporous silicas and did not leach from the supports during the reaction.

3.3.2. Asymmetric dihydroxylation. Similar to asymmetric epoxidation, asymmetric dihydroxylation of alkenes catalyzed by cinchona alkaloid ligand and osmium tetroxide[95] also provides two chiral centres in one reaction process. Due to high cost of these expensive chiral ligands, such as cinchona alkaloid, immobilization of them on supports is a favorable way of ensuring its recycling.

An early work was reported by Crudden group.[96] In their work, a chiral cinchona alkaloid-derivated siloxane, obtained by treatment of a cinchona alkaloid derivative with $HSi(OEt)_3$ in the presence of H_2PtCl_6, was grafted directly onto mesoporous SBA–type material to afford the chiral supported ligand **7** (Scheme 26). For comparison, this chiral ligand was also anchored on the surface of silica gel. The dihydroxylation of methyl cinnamate was carried out in the presence of K_2OsO_4. It was found that both supported ligands gave the nearly same enantioselectivity as the homogeneous counterpart, and that the SBA–based ligand provided a slightly higher yield than either the homogeneous ligand or the silica gel–supported ligand. Furthermore, the ligand supported on the SBA–type silica could be recovered and reused several times without any obvious loss of catalytic activity or enantioselectivity.

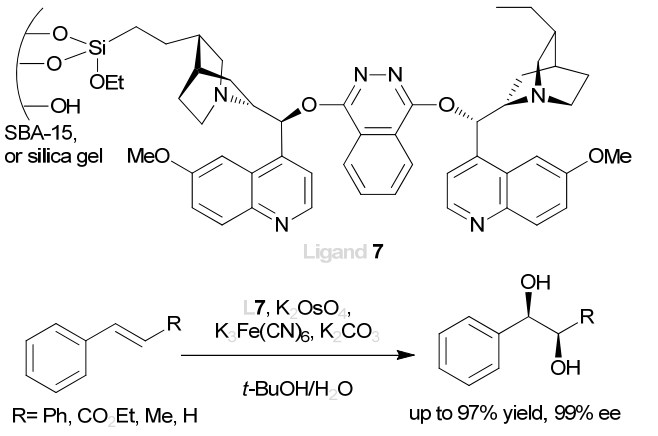

Scheme 26 Structure of supported ligand **7** and its catalytic application.

At almost the same time, Kim and co–workers[97] also grafted successfully various cinchona alkaloid ligands on mesoporous SBA–15 to prepare the supported ligands **8**–**10** (Figure 6). These supported ligands were efficient in the asymmetric dihydroxylation of alkenes in the presence of OsO_4.

It was also found that the reaction with ligand **10** gave the best enantioselectivity, which was comparable to that obtained with its homogeneous counterpart. This indicated the importance of the linker length for optimal geometry in the transition state of the dihydroxylation, in which a longer linker may provide a greater degree of freedom for methoxyquinoline in the channels of SBA–15. Due to the lack of a dimeric effect, the enantioselectivity with the ligand **8** was lower than those obtained with the ligands **9** and **10**. To facilitate subsequent recycling of the catalyst, the authors also immobilized the cinchona alkaloid on magnetic mesocellular mesoporous silica, thereby providing a filtration–free recyclable chiral supported ligand.[98] This magnetically recoverable ligand could be separated from the reaction system using an external magnet and reused at least eight times without any obvious loss of the enantioselectivity.

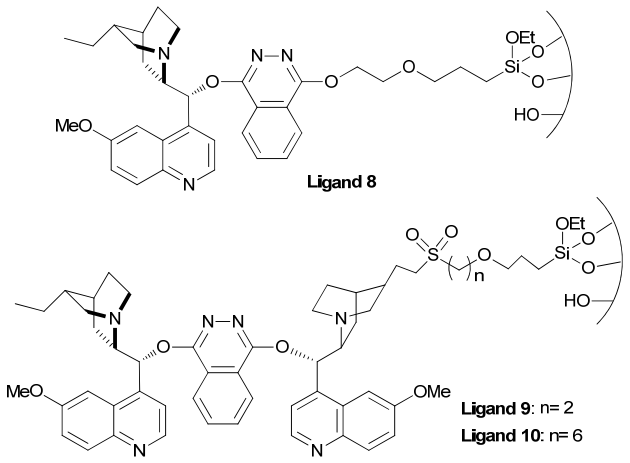

Figure 6 Structures of supported ligands **8**–**10**.

3.3.3. Asymmetric oxidation of sulfide to sulfoxide. Besides the oxidation of alkenes discussed above, enantioselective oxidation of sulfide to chiral sulfoxide had also been involved. The first example catalyzed by a mesoporous silica–based chiral catalyst was reported by Iwamoto group.[99,100] In this work, they reported a series of metal–containing MCM–41 catalysts by the template–ion–exchange method. These metal compounds included nitrate (Al, Cr, Fe, Co), acetate (Mn, Cu, Zn), $NH_2[TiO(C_2O_4)_2]$ and $ZrO(NO_3)_2$. Oxidations of methyl phenyl sulfide were performed at room temperature, and the results showed that Ti–MCM–41 was the best catalyst and H_2O_2 was the most efficient oxidant. Based on the obtained results, tartaric acid and its derivatives (**L11**–**18**, Figure 7) were screened for the asymmetric oxidation of sulfide to sulfoxide. It was found that both two COOH and OH groups of tartaric acid were both essential for the asymmetric oxidation, in which chiral **L11** and **L12** gave almost the same high *ee* values, while those with one COOH and OH, or the others had no enantioselectivity.

Later, García and co–workers[101] reported the preparation of chiral tartramide–functionalized PMO and its application in asymmetric sulfoxidation. As shown in Scheme 27, the bis-silylated chiral tartramide ligand obtained from the reaction of (*N*-methyl-3-aminopropyl)trimethoxysiloxane and chiral protected dimethyl tartrate was co–condensed with TEOS to prepare MCM–41–type PMO. The chiral PMO-supported ligand **19** was then synthesized through the treatment of an ethanolic solution of hydrochloric acid. For comparison, a bis-silylated tartramide was also grafted onto pure MCM–41 material as a reference ligand. Finally, the heterogeneous catalysts were generated by an *in situ* complexation with titanium isopropoxide, and were used for the asymmetric oxidation of methyl phenyl sulfide with cumyl hydroperoxide as an oxidant. The results showed that the PMO–based catalyst exhibited better catalytic performance than the grafted catalyst.

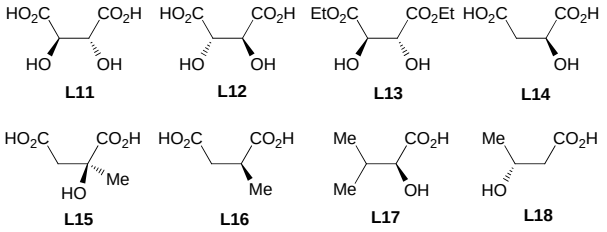

Figure 7 Structures of supported ligands **11**–**18**.

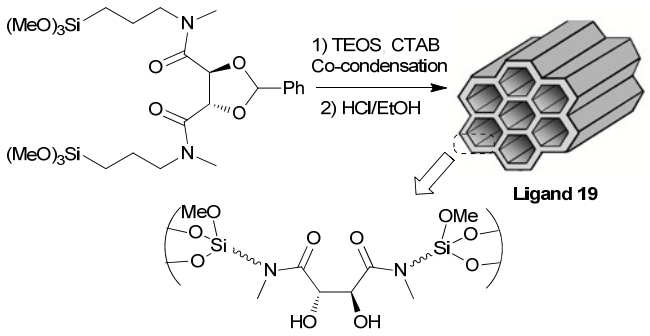

Scheme 27 Preparation of supported ligand **19**.

Besides the use of tartaric acid and its derivatives, a SBA–15–supported Ti–based heterogeneous catalyst have recently been developed through the use of chiral BINOL as a ligand. Halligudi group[102] immobilized a chiral Ti–BINOL complex on an ionic–liquid–modified SBA–15 by electrostatic interaction. This heterogeneous catalyst exhibited moderate catalytic activity (54-62% yields) and excellent enantioselectivity (up to 99.9% *ee*) as same as those obtained with its homogeneous counterpart (99% *ee*). In addition, the supported catalyst could be recovered and reused at least eight times without any loss of enantioselectivity. Later, Khedher and co–workers[103] also immobilized a chiral vanadyl salen complex on amino–functionalized mesoporous silica through a post–modification method. This supported catalyst exhibited catalytic efficiency for the asymmetric oxidation of methyl phenyl sulfide using H_2O_2 as an oxidant.

Very recently, Hosseini-Monfared and co-workers[104] synthesized a chiral diethyl tartrate-based ligand, which was then grafted onto mesoporous silica support (SBA-15) to afford

heterogeneous catalyst **33** through the complexation of as-prepared supported ligand and $MnCl_2$ (Figure 8). The heterogeneous catalyst **33** exhibited excellent conversion and enantioselectivity (>99% ee) in the asymmetric oxidation of thioanisole (PhSMe). Compared to its homogeneous counterpart, the heterogeneous catalyst **33** is more stable and could be recycled four times without any significant loss of its reactivity.

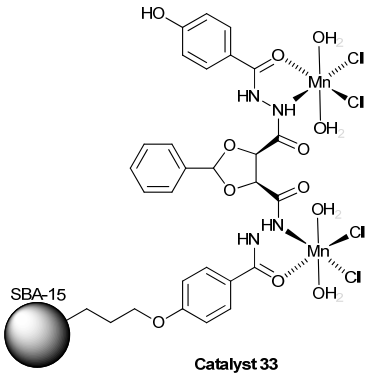

Figure 8 Structure of catalyst **33.**

3.3.4. Asymmetric oxidative kinetic resolution. Besides the asymmetric reduction of ketones discussed above, only two examples were used to asymmetric oxidative kinetic resolution of racemic alcohols through the use of chiral transition–metal-based heterogeneous catalysts. First work was reported by Jones and co–workers[105]. As shown in Scheme 28, a chiral V-based heterogeneous catalyst could be constructed through the direct immobilization of tridentate Schiff–base vanadium complex on mesoporous silica SBA–15, providing the heterogeneous catalyst **34**. In the asymmetric oxidative kinetic resolution of ethyl mandelate in both dry acetone and dry acetonitrile, the resolution was complete in 11 h, reaching 99% conversion of *S*-ethyl mandelate and 98% *ee* of *R*-ethyl mandelate (total conversion *S*+*R*: 49%). Furthermore, they also found that the catalyst **34** supported on mesoporous silica was more selective than those with polymer-support, even that with its homogeneous counterpart, suggesting that the nature of the support could influence the reaction selectivity. However, due to cleavage of the imine functionality in the ligand, the activity of catalyst **34** reduced with each run during recycling experiments.

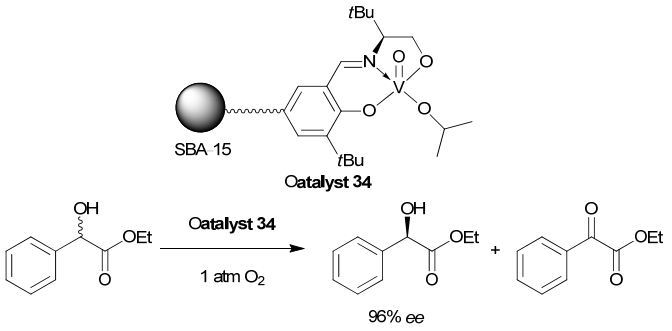

Scheme 28 Structure of catalyst **34** and its catalytic application.

Another example was a chiral Mn-based heterogeneous catalyst. Similar to their reported heterogeneous catalyst[102], Halligudi and co–workers[106] found that a chiral Mn(salen) complex onto ionic–liquid–modified SBA–15 by electrostatic interaction also enabled effective asymmetric oxidative kinetic resolution of racemic alcohols, in which the reaction with up to 65% conversion and 99% *ee* could be obtained.

3.4 Asymmetric Diels–Alder (D–A) reaction

The D–A reaction is an efficient C–C bond–forming reaction, providing cyclic compounds with a double bond and two newly formed C–C single bonds, which can also be extended to heterocyclic compounds. With the development of asymmetric catalysis, many complexes of Lewis acidic metals with chiral ligands had been developed to control the *endo*/*exo* diastereoselectivity as well as the enantioselectivity. Recently, a few examples of the use of the immobilization of chiral complexes on mesoporous siliceous materials for D–A reactions have also been explored.

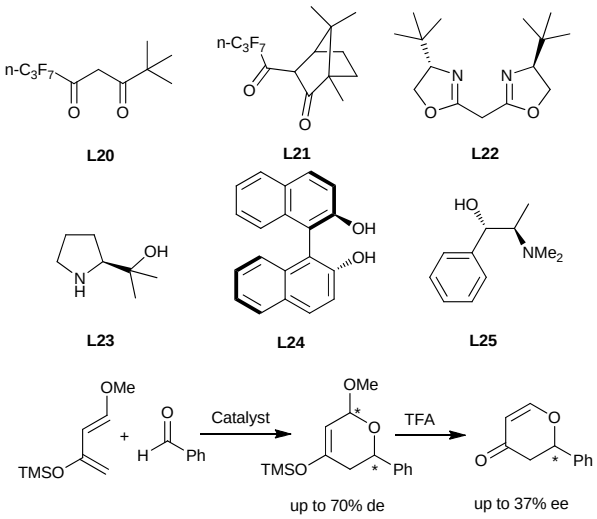

Scheme 29 Structures of supported ligands **20–25** and catalytic asymmetric hetero–D–A reaction.

An early work was reported by Gerstberger and Anwander.[107] They grafted the yttrium complex onto mesoporous silica MCM–41, and the Y centres were then modified with different chiral supported ligands **20–25** through surface–mediated ligand–exchange reactions, providing a series of chiral heterogeneous catalysts. These heterogeneous catalysts were applied for the asymmetric hetero–D–A cyclization of *trans*-1-methoxy-3-trimethylsilyloxy-1,3-butadiene with benzaldehyde, as shown in Scheme 29. It was found that most of the supported catalysts gave the products in higher yields but with lower enantioselectivities than the homogeneous catalysts.

Another example was reported by Kim and co–workers.[108] In their work, they prepared a chiral supported ligand **26** (Scheme 30) for D–A reaction by immobilizing a chiral

bis(oxazoline) on MCF. In this case, a chloropropyl linker was grafted onto the mesoporous silica support MCF, which was then reacted with chiral bis(oxazoline) ligand to generate the precursor of the supported ligand. The free SiOH groups were then protected by TMS groups to provide the chiral supported ligand, and finally the heterogeneous catalyst was obtained by an *in situ* complexation with $Cu(OTf)_2$. Similarly, this copper bis(oxazoline) complex could also be electrostatically bound within Y-type zeolite and mesoporous materials MCM–41, Al–SBA–15, and MSU–2 reported by Hutchings and co–workers.[109] These heterogeneous catalysts were used for the D–A reaction of (*E*)-ethyl 2-oxo-3-pentenoate and vinyl ethyl ether. The results showed that the catalyst immobilized on Y-type zeolite gave the highest *ee* value. Such an *ee* value (40% *ee*) was much higher than that (20% *ee*) of its homogeneous counterpart, suggesting the positive effect of the steric bulk around the metal centre.

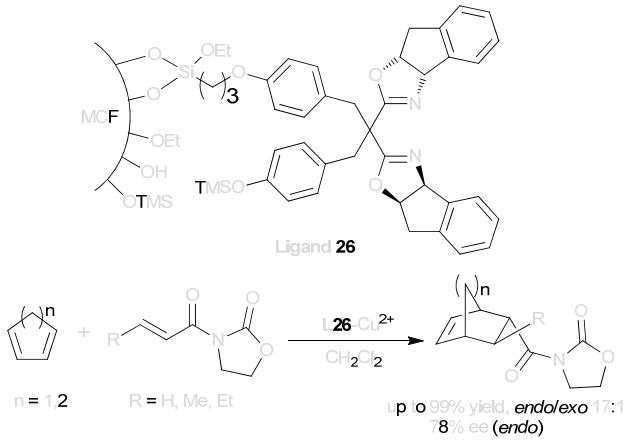

Scheme 30 Structure of supported ligand **26** and the D–A reaction catalyzed by **L26**–Cu^{2+}.

3.5 Asymmetric addition of dialkylzinc to aldehydes

Besides the asymmetric reduction of prochiral ketones and the asymmetric oxidative kinetic resolution of racemic alcohols discussed above, ordered mesoporous silica–supported chiral transition–metal-based catalysts had also been applied to the asymmetric addition of dialkylzinc to aldehydes to synthesize chiral alcohols.

An early work was reported by Abdi group[110]. They used a post–grafting method to anchor a chiral BINOL-derived siloxane on the ordered mesoporous silica MCM–41 and SBA–15, providing the supported ligand **27** (Scheme 31). In order to avoid the interaction of silanol groups on solid supports and Ti cation, the silanol groups were protected by TMS groups. The heterogeneous catalysts generated by an *in situ* complexation with $Ti(OiPr)_4$ was applied to the asymmetric addition of dialkylzinc to aromatic aldehydes. However, the heterogeneous catalysts displayed much poorer activity when was compared to the homogeneous catalyst. Interestingly, they found that the SBA–15–supported heterogeneous catalyst had higher conversion and better enantioselectivity than that obtained with MCM–41–supported heterogeneous catalyst. This observation indicated that the larger pore size of SBA–15 support enabled to increase the diffusion of reactants, leading to a high catalytic efficiency. Based on the this finding, they further grafted the chiral BINOL-derivated siloxane on an a MCF support with a larger pore size than SBA–15.[111] As expected, the MCF–supported chiral Ti-based catalyst displayed highly catalytic activity and up to 94% *ee* in the asymmetric addition of diethylzinc to various aldehydes. Furthermore, this catalyst could be reused in multiple catalytic runs without loss of enantioselectivity.

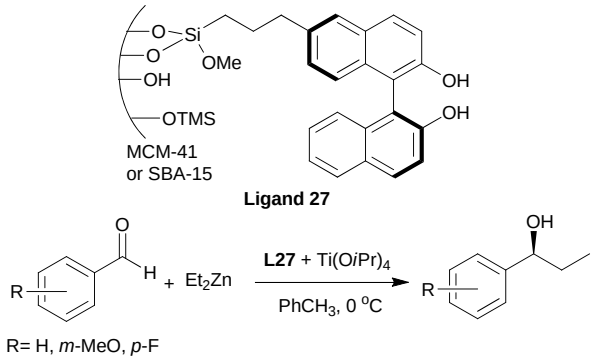

Scheme 31 Structure of supported ligand **27** and the reaction catalyzed by **L27**–Ti.

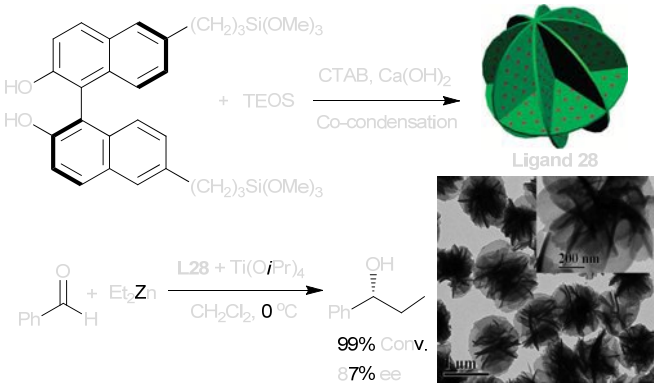

Scheme 32 Preparation of supported ligand **28** and the reaction catalyzed by **L28**–Ti.

Another work was reported by Li and co–workers.[112] In this work, they utilized a 3D flower–like mesoporous architectures constructed from ultra–thin perpendicularly aligned mesoporous nanoflakes as supports to construct a chiral Ti-based heterogeneous catalyst. As shown in Scheme 32, the supported ligand **28** was synthesized by the co–condensation of BINOL-derivated siloxane and TEOS in the presence of $Ca(OH)_2$ and CTAB as dual templates. The existence of uniformly distributed spherical 3D flower–like arrays and mesopores on the nanoflakes could be clearly observed in a transmission electron microscopy (TEM) image. The heterogeneous catalyst generated by an *in situ* complexation of ligand **28** with $Ti(OiPr)_4$ displayed high catalytic activity and 87% *ee* value in the asymmetric addition of diethylzinc to benzaldehyde, which was attributed to its ultra–thin nanoflake building blocks with perpendicularly aligned mesochannels.

3.6 Asymmetric nucleophilic addition

Differed from asymmetric addition of dialkylzinc to aldehydes, a few examples through the use of ordered mesoporous silica–supported chiral transition–metal–based catalysts had also expanded to asymmetric Michael additions and asymmetric nitro–Mannich reaction.

Recently, Liu and co–workers[113,114] reported the PMO–supported chiral Ni-based catalysts **35** for asymmetric Michael addition of 1,3-dicarbonyl compounds to nitroalkenes. As shown in Scheme 33, the co–condensation of chiral *N*,*N*-dibenzylcyclohexyldiamine–derivated siloxane and 1,4-bis(triethoxysilyl)benzene (or 1,2-bis(triethoxysilyl)ethene) provided chiral DACH–functionalized PMOs. Catalysts could be obtained successfully by direct complexation with $NiBr_2$ in the presence of chiral *N*,*N*-dibenzylcyclohexyldiamine. Both heterogeneous catalysts possessed the ordered hexagonal pore mesostructures, which exhibited excellent catalytic activities (up to 99% conversion) and enantioselectivities (up to 99% *ee*) in asymmetric Michael addition of malonates to nitroalkenes. Such an enantioselectivity was comparable to 94% *ee* of its homogeneous catalyst. In addition, the heterogeneous chiral catalysts could be easily recovered and reused for up to nine times without obvious loss of their enantioselectivities.

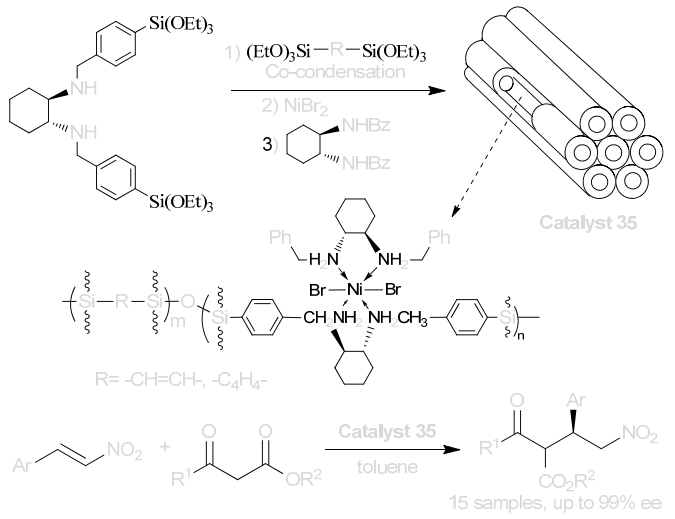

Scheme 33 Preparation of catalyst **35** and its catalytic application.

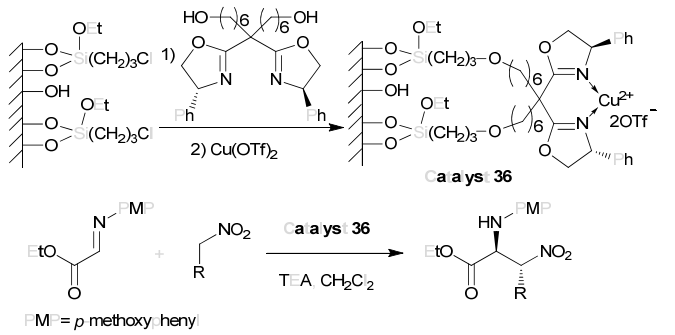

Scheme 34 Preparation of catalyst **36** and its catalytic application.

Another example was reported by Kim and co–workers that had been demonstrated as an efficient heterogeneous catalyst in asymmetric D–A reactions.[108] Later, they found that this chiral Cu-based heterogeneous catalyst could also catalyze the asymmetric nitro–Mannich reaction.[115] As shown in Scheme 34, a chiral bis(oxazoline) ligand was anchored on SBA–15, which could be coordinated with $Cu(OTf)_2$ to afford the heterogeneous catalyst **36**. Although catalyst **36** needed longer reaction times for catalytic performance, its enantioselectivity was comparable to that obtained with its homogeneous counterpart in the asymmetric nitro–Mannich reactions. The result of recycling experiments indicated that a comparable level of yield was maintained after recycled five times. However, enantioselectivity dropped significantly, which was attributed to the leaching of the copper metal from the supported ligand-metal complex.

3.7 Asymmetric Henry reaction and cyanosilylation of benzaldehyde

In addition to asymmetric Michael additions and asymmetric nitro–Mannich reaction, an ordered mesoporous silica–supported chiral Cu–based catalyst had also been applied to asymmetric Henry reaction.[116] In this work, a chiral bis(oxazoline) ligand was anchored on an alkynyl–functionalized magnetic mesoporous silica through a click reaction. Chiral heterogeneous catalyst could be obtained by an similar *in situ* complexation with $Cu(OAc)_2$, which produced the chiral products with 33% to 97% yields and 55% to 86% *ee* values in asymmetric Henry reactions of nitromethane with various aldehydes. It was noteworthy that the heterogeneous catalyst could be easily separated from the reaction mixture with an external magnet and reused several times without significant loss of reactivity or enantioselectivity. Similarly, Abdi group[117] also reported a SBA–15–supported (or MCF–supported) chiral Cu–based heterogeneous catalyst **37** (Scheme 35). It was found that catalyst **37** exhibited remarkably high catalytic activity (up to 97% yield) and enantioselectivity (up to 99% *ee*) in the asymmetric Henry reactions under mild conditions.

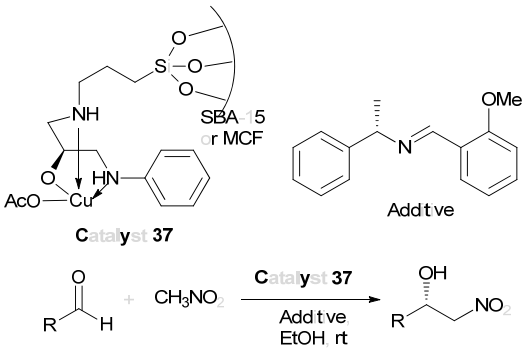

Scheme 35 Structure of catalyst **37** and its catalytic application.

In addition, through thio-ene click reactions, Corma and co–workers[118] also reported a series of chiral V-based

heterogeneous catalysts by the anchor of VO(salen) complex on thio–functionalized amorphous silica, delaminated zeolite, MCM–41, and MCM–41–like PMO. It was found that MCM–41–like PMO–supported had much higher catalytic activities but lower enantioselectivities than that obtained with MCM–41–supported heterogeneous catalyst in the asymmetric trimethylsilylcyanation of benzaldehydes.

Also, MCM–41–supported Ti–based heterogeneous catalysts developed by the Kim group[119] could be applied to asymmetric trimethylsilylcyanation of benzaldehyde. In their work, several Ti(salen) complexes were immobilized on ordered mesoporous silica MCM–41 through a post–grafting method or an electrostatic interaction. The heterogeneous catalysts produced the chiral products with 23% to 40% conversion and 43% to 93% *ee* values in the asymmetric trimethylsilylcyanation of benzaldehyde.

Furthermore, by the use the entrapment method, chiral VO(salen) complex could be encapsulated within SBA–16 reported by Li and co–workers,[120] which was similar to their previous report.[51] This heterogeneous catalyst exhibited high catalytic activity and enantioselectivity in the asymmetric trimethylsilylcyanation of benzaldehydes, which were comparable to those of its homogeneous counterpart. Interestingly, it was found the different solvent effect for the solid catalyst from the homogeneous counterpart, which is probably due to the altered microenvironment of VO(Salen) complex encapsulated in the nanocage of SBA-16. Moreover, the catalyst could be recovered and reused at least six times without obvious loss of activity or enantioselectivity.

3.8 Asymmetric kinetic resolution of racemic epoxides

Besides the asymmetric oxidative kinetic resolution of racemic alcohols discussed above, the use of chiral transition–metal-based heterogeneous catalysts was also used to asymmetric kinetic resolution of racemic epoxides.

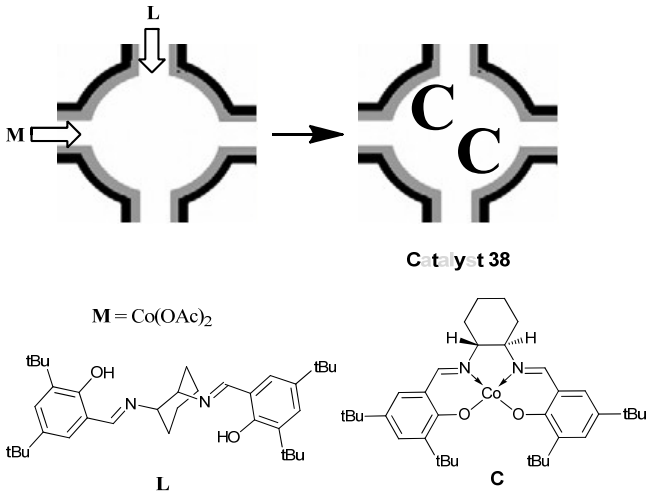

Scheme 36 Preparation of catalyst **38**.

Li and co–workers[121] developed a SBA-16-supported chiral Co-based heterogeneous catalyst **38** and applied it to the asymmetric kinetic resolution of racemic epoxides. As shown in Scheme 36, in this work, they took use of their previous procedure[51] to modify the pore entrance size of SBA–16 by phenyltrimethoxysiloxane. chiral Co(salen) complex was then assembled in the mesoporous cage of SBA–16 through the "ship in a bottle" method, furnishing the heterogeneous chiral catalyst **38**. After oxidation of Co(II)(salen) to Co(III)(salen), the heterogeneous catalyst was used to catalyze the asymmetric ring–opening of racemic epoxides. The results showed that the heterogeneous catalyst exhibited similar enantioselectivity but slightly lower activity in generating the diol compared with its homogeneous counterpart. In addition, this heterogeneous catalyst could be easily recovered and reused at least nine times with maintained enantioselectivity, albeit with slightly decreased activity.

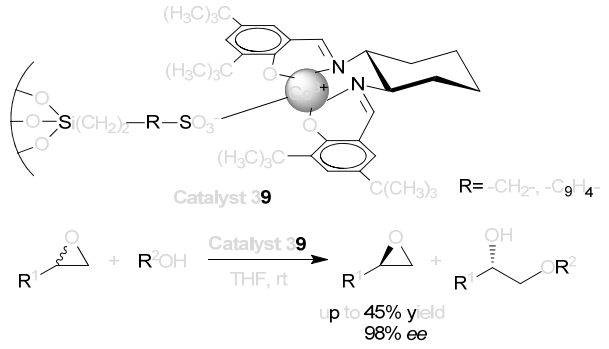

Scheme 37 Structure of catalyst **39** and its catalytic application.

Later, Kim group[122] immobilized the same Co(salen) complex as in Li's catalyst[121] through electrostatic interaction with sulfonic acid linkages on ordered mesoporous SBA–16 silica, thereby furnishing catalyst **39** (Scheme 37). Asymmetric ring–opening reactions of racemic epoxides by nucleophiles such as water and phenol derivatives were conducted in the presence of catalyst **39**. The results showed that the catalyst exhibited remarkable activities and enantioselectivities in these reactions, producing chiral terminal epoxides. Furthermore, the heterogeneous catalyst could be reused several times without further treatment after reaction without significant loss in its activity.

3.9 Other applications

Besides the asymmetric D–A, nitro–Mannich, and Henry reactions discussed above, supported copper–chiral bis(oxazoline) complexes have also been used to catalyze enantioselective Friedel-Crafts hydroxyalkylations, as described by Corma and co–workers[123]. A copper–bis(oxazoline) complex with a terminal ethylene unit was anchored on mercapto–functionalized MCM–41. This catalyst showed good activity and high enantioselectivity in the Friedel-Crafts hydroxyalkylation of 1,3–dimethoxybenzene with 3,3,3–trifluoropyruvate (Scheme 38). However, the enantioselectivity of the reaction catalyzed by the MCM–41–based catalyst was lower than that of the reaction catalyzed by a silica gel–based

catalyst due to the negative influence of the residual free OH groups on MCM–41.

Later, Silva and co-worker[124] found that the copper-chiral aza-bis(oxazoline) complex could be also anchored onto ordered mesoporous silicas (SBA-15, SPSi, HMS) and their carbon replicas (CMK-3, SPC) to provide a series of chiral Cu-based heterogeneous catalysts. Generally, theses heterogeneous catalysts were more active and enantioselective in the asymmetric cyclopropanation of styrene than the corresponding homogeneous counterpart under similar experimental conditions (heterogeneous enantioselectivity with %ee *cis* and %ee *trans* of 72 and 80 versus homogeneous enantioselectivity with %ee *cis* and %ee *trans* of 41 and 44), indicating a positive immobilization effect. Interestingly, it was found that the materials pH was an important factor not only in the copper-chiral aza-bis(oxazoline) complex anchoring yields, but also in their catalytic performance, in which less acidic surfaces (SPSi and CMK-3) yielded heterogeneous catalysts with high styrene conversion and enantioselectivity.

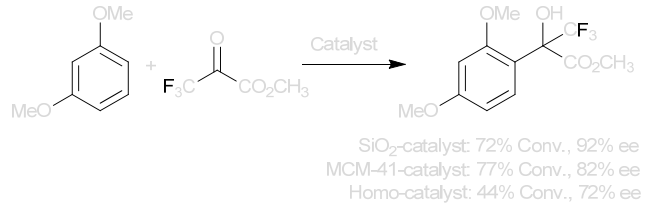

Scheme 38 Enantioselective Friedel–Crafts hydroxyalkylation.

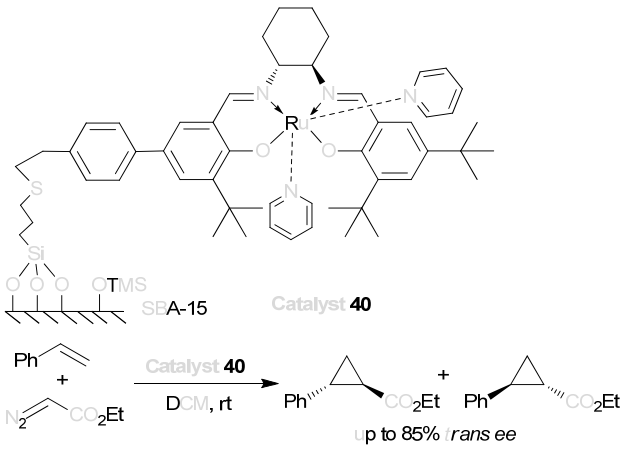

Scheme 39 Structure of catalyst **40** and its application in asymmetric cyclopropanation.

Also, Jones et al.[125] developed an SBA–15–supported Ru(salen)-based heterogneous catalyst **40** (Scheme 39) for the asymmetric cyclopropanation of alkenes. The salen ligand was silanized using a thiol-ene click reaction with γ–Mercaptopropyltrimethoxysiloxane (MPTMS), and was then grafted onto ordered mesoporous SBA–15 to provide an Ru(salen)–functionalized support. The free OH groups on the functionalized SBA–15 were protected by TMS groups, and then Ru was chelated by the supported ligand to afford the final catalyst. The activity of catalyst **40** in asymmetric cyclopropanation reactions was evaluated. The results indicated that the SBA–15–based catalyst generated the desired products in high yields and with moderate enantioselectivities (85% *ee*), which was much lower than that of its homogeneous counterpart (99% *ee*). Compared to polymer–supported catalysts, it gave lower enantioselectivity, possibly due to adverse reaction or steric hindrance with the silica surface.

Interestingly, Somorjai and co-workers[126] developed an heterogeneous catalyst **41**, which was prepared by encapsulating metallic nanoclusters in chiral self-assembled monolayer (SAM), immobilized on mesoporous SiO_2 support. As shown in Scheme 40, heterogeneous catalyst **41** provided up to 51% enantioselectivity with high diastereoselectivity in asymmetric cyclopropanation of olefin. This research highlights that asymmetric reactions could be catalyzed by Au clusters embedded in chiral SAM, in which the synergetic effect of the catalytically active metallic sites and the surrounding chiral SAM leads to a highly active mesoscale heterogeneous catalyst with the improved enantioselectivity due to the formation of a hydrogenbonding network in the chiral SAM.

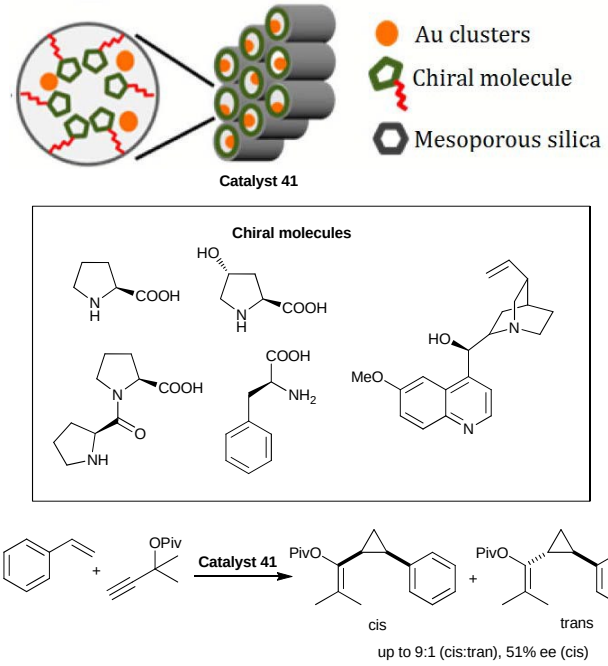

Scheme 40 Structure of catalyst **41** and its application in asymmetric cyclopropanation.

Very recently, Adint and Landis[127] covalently anchored enantiopure bis-3,4-diazaphospholanes (BDPs) that had been functionalized with carboxylic acids on polymer and silica supports providing heterogeneous catalyst **42**. As shown in Scheme 41, catalysts **42** were used to catalyze asymmetric hydroformylations. Compared with the catalyst supported on Tentagel resin, the SBA–15–bound catalyst exhibited inferior activity and enantioselectivity.

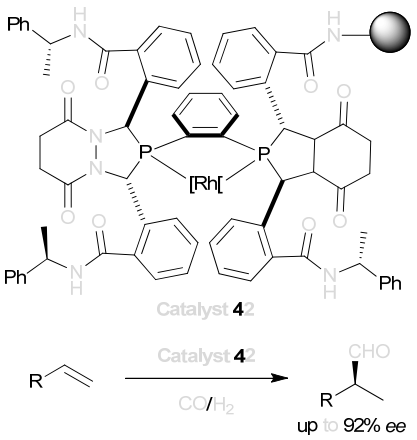

Scheme 41 Structure of catalyst **42** and its catalytic application.

4 Summary and outlook

Developments of mesoporous silica–supported chiral transition–metal–based catalysts and their applications in various asymmetric transformations have obtained great achievements in the past few decades. Numerous mesoporous silica–supported chiral transition–metal–based catalysts have been reported and some of them have showed good catalytic activity and enantioselectivity for various kinds of asymmetric reactions. However, there are still some challenges for future researches and practical applications. Firstly, the exact mechanisms of asymmetric reactions catalyzed by these mesoporous silica–supported chiral transition–metal–based catalysts are not very clear. Although lots of heterogeneous catalysts with increased catalytic activity and enantioselectivity with supported chiral catalysts compared with the corresponding homogeneous counterparts has frequently been obtained, the origin of morphological effect, confinement effect, synergistic effect is still unclear completely. Thus, more detail insights are necessary, which would be very helpful for the further design of mesoporous silica–supported chiral transition–metal–based catalysts. Secondly, characterization methods need to be improved. Although several characterization methods, such as scanning electron microscopy (SEM), transmission electron microscopy (TEM), X–ray photoelectron spectroscopy (XPS), atomic force microscopy (AFM), and X–ray diffraction (XRD), have been well established for mesoporous materials, they are not entirely adequate. But, in a typical asymmetric reaction, the relationship of the structural morphology of support and electronic structures of active species is complicated. Therefore, the development of better characterization technique, such as synchrotron-based X-ray absorption, *in situ* synchrotron-based XPS, and IR microspectroscopy methods, is essential for investigation of the interactions. Finally, the practical applications of mesoporous silica–supported chiral catalysts are still at an early stage. Thus, highly active and enantioselective mesoporous silica–supported chiral transition–metal–based catalysts need to be further explored, whilst facile, scalable, and reliable synthetic strategies for construction of mesoporous silica–supported chiral transition–metal–based catalysts need to be further enriched. In particular, by taking use of the advantages of functionalized mesoporous materials, development of multifunctional catalysts and exploration of cascade asymmetric reactions to overcome of barriers of homogeneous catalyst, achieving high stability, sustainability, and environmentally friendly mesoporous silica-supported transition–metal–based catalysts for industrial applications are still unmet challenges for the future endeavors.

Acknowledgements

We are grateful to China NSF (21402120), the Shanghai Sciences and Technologies Development Fund (13ZR1458700 and 12nm0500500), the Shanghai Municipal Education Commission (14YZ074, 13CG48, Young Teacher Training Project), Specialized Research Fund for the Doctoral Program of Higher Education (20133127120006).

Notes and references

Key Laboratory of Resource Chemistry of Ministry of Education, Shanghai Key Laboratory of Rare Earth Functional Materials, Shanghai Normal University, Shanghai 200234, P. R. China. Tel: +86 21 64321819; E–mail: ghliu@shnu.edu.cn.

1. H. Nishiyama and J. Ito, *Chem. Commun.*, 2010, **46**, 203-212.
2. T. Katsuki, *Chem. Soc. Rev.*, 2004, **33**, 437-444.
3. J.-P. Genet, T. Ayad and V. Ratovelomanana-Vidal, *Chem. Rev.*, 2014, **114**, 2824-2880.
4. T. T. L. Au-Yeung and A. S. C. Chan, *Coord. Chem. Rev.*, 2004, **248**, 2151-2164.
5. R. Noyori, *Angew. Chem., Int. Ed.*, 2002, **41**, 2008-2022.
6. H. A. McManus and P. J. Guiry, *Chem. Rev.*, 2004, **104**, 4151-4202.
7. G. Helmchen and A. Pfaltz, *Acc. Chem. Res.*, 2000, **33**, 336-345.
8. A. G. Doyle and E. N. Jacobsen, *Chem. Rev.*, 2007, **107**, 5713-5743.
9. S. J. Connon, *Chem. Commun.*, 2008, 2499-2510.
10. V. Cesar, S. Bellemin-Laponnaz and L. H. Gade, *Chem. Soc. Rev.*, 2004, **33**, 619-636.
11. C. T. Kresge, M. E. Leonowicz, W. J. Roth, J. C. Vartuli and J. S. Beck, *Nature*, 1992, **359**, 710-712.
12. Z. Li, J. C. Barnes, A. Bosoy, J. F. Stoddart and J. I. Zink, *Chem. Soc. Rev.*, 2012, **41**, 2590-2605.
13. A. Sayari and S. Hamoudi, *Chem. Mater.*, 2001, **13**, 3151-3168.
14. Y. Wan and Zhao, *Chem. Rev.*, 2007, **107**, 2821-2860.
15. M. Campanati, G. Fornasari and A. Vaccari, *Catal. Today*, 2003, **77**, 299-314.
16. T. Cheng, D. Zhang, H. Li and G. Liu, *Green Chem.*, 2014, **16**, 3401-3427.
17. M. Heitbaum, F. Glorius and I. Escher, *Angew. Chem., Int. Ed.*, 2006, **45**, 4732-4762.
18. H. Ngo and W. Lin, *Top. Catal.*, 2005, **34**, 85-92.
19. J. M. Thomas and R. Raja, *Acc. Chem. Res.*, 2008, **41**, 708-720.

20. J. M. Fraile, J. I. García and J. A. Mayoral, *Chem. Rev.*, 2008, **109**, 360-417.
21. J. Jamis, J. R. Anderson, R. S. Dickson, E. M. Campi and W. R. Jackson, *J. Organomet. Chem.*, 2000, **603**, 80-85.
22. J. Jamis, J. R. Anderson, R. S. Dickson, E. M. Campi and W. R. Jackson, *J. Organomet. Chem.*, 2001, **627**, 37-43.
23. A. Crosman and W. F. Hoelderich, *J. Catal.*, 2005, **232**, 43-50.
24. H. H. Wagner, H. Hausmann and W. F. Hölderich, *J. Catal.*, 2001, **203**, 150-156.
25. A. Crosman and W. F. Hoelderich, *Catal. Today*, 2007, **121**, 130-139.
26. C. Simons, U. Hanefeld, I. W. C. E. Arends, R. A. Sheldon and T. Maschmeyer, *Chemi.–Eur. J.*, 2004, **10**, 5829-5835.
27. W. P. Hems, P. McMorn, S. Riddel, S. Watson, F. E. Hancock and G. J. Hutchings, *Org. Biomol. Chem.*, 2005, **3**, 1547-1550.
28. R. Sayah, E. Framery and V. Dufaud, *Green Chem.*, 2009, **11**, 1694-1702.
29. C. del Pozo, A. Corma, M. Iglesias and F. Sanchez, *Green Chem.*, 2011, **13**, 2471-2481.
30. S. Sahoo, P. Kumar, F. Lefebvre and S. B. Halligudi, *J. Catal.*, 2008, **254**, 91-100.
31. C. Pérez, S. Pérez, G. A. Fuentes and A. Corma, *J. Mol. Catal. A: Chem.*, 2003, **197**, 275-281.
32. M. D. Jones, R. Raja, J. M. Thomas, B. F. G. Johnson, D. W. Lewis, J. Rouzaud and K. D. M. Harris, *Angew. Chem.*, 2003, **115**, 4462-4467.
33. A. Ghosh and R. Kumar, *J. Catal.*, 2004, **228**, 386-396.
34. B. Kesanli and W. Lin, *Chem. Commun.*, 2004, 2284-2285.
35. D. J. Mihalcik and W. Lin, *Angew. Chem.*, 2008, **120**, 6325-6328.
36. D. J. Mihalcik and W. Lin, *ChemCatChem*, 2009, **1**, 406-413.
37. S. Sahoo, P. Kumar, F. Lefebvre and S. B. Halligudi, *J. Mol. Catal. A: Chem.*, 2 007, **273**, 102-108.
38. L.-L. Lou, X. Peng, K. Yu and S. Liu, *Catal. Commun.*, 2008, **9**, 1891-1893.
39. L.-L. Lou, Y. Dong, K. Yu, S. Jiang, Y. Song, S. Cao and S. Liu, *J. Mol. Catal. A: Chem.*, 20 10, **333**, 20-27.
40. P. Wang, X. Liu, J. Yang, Y. Yang, L. Zhang, Q. Yang and C. Li, *J. Mater. Chem.*, 2009, **19**, 8009-8014.
41. T. Seki, K. McEleney and C. M. Crudden, *Chem. Commun.*, 2012, **48**, 6369-6371.
42. Y. Huang, S. Xu and V. S. Y. Lin, *ChemCatChem*, 2011, **3**, 690-694.
43. G. Liu, J. Wang, T. Huang, X. Liang, Y. Zhang and H. Li, *J. Mater. Chem.*, 2010, **20**, 1970-1975.
44. G. Liu, M. Yao, J. Wang, X. Lu, M. Liu, F. Zhang and H. Li, *Adv. Synth. Catal.*, 2008, **350**, 1464-1468.
45. G. Liu, M. Liu, Y. Sun, J. Wang, C. Sun and H. Li, *Tetrahedron: Asymmetry*, 2009, **20**, 240-246.
46. P. N. Liu, P. M. Gu, F. Wang and Y. Q. Tu, *Org. Lett.*, 2003, **6**, 169-172.
47. P. N. Liu, J. G. Deng, Y. Q. Tu and S. H. Wang, *Chem. Commun.*, 2004, 2070-2071.
48. P.-N. Liu, P.-M. Gu, J.-G. Deng, Y.-Q. Tu and Y.-P. Ma, *Eur. J. Org. Chem.*, 2005, **2005**, 3221-3227.
49. X. Huang and J. Y. Ying, *Chem. Commun.*, 2007, 1825-1827.
50. J. Li, Y. Zhang, D. Han, Q. Gao and C. Li, *J. Mol. Catal. A: Chem.*, 2009, **298**, 31-35.
51. H. Yang, J. Li, J. Yang, Z. Liu, Q. Yang and C. Li, *Chem. Commun.*, 2007, 1086-1088.
52. R. Liu, T. Cheng, L. Kong, C. Chen, G. Liu and H. Li, *J. Catal.*, 2013, **307**, 55-61.
53. D. Zhang, X. Gao, T. Cheng and G. Liu, *Sci. Rep.*, 2014, **4**, 5091.
54. D. Zhang, J. Xu, Q. Zhao, T. Cheng and G. Liu, *ChemCatChem*, 2014, **6**, 2998-3003.
55. M. Jin, M. Sarkar, V. B. Takale and S. Park, *Bull. Korean Chem. Soc.*, 2005, **26**, 1671-1672.
56. S. Parambadath and A. P. Singh, *Catal. Today*, 2009, **141**, 161-167.
57. D. Jiang, Q. Yang, J. Yang, L. Zhang, G. Zhu, W. Su and C. Li, *Chem. Mater.*, 2005, **17**, 6154-6160.
58. D. Jiang, J. Gao, Q. Yang, J. Yang and C. Li, *Chem. Mater.*, 2006, **18**, 6012-6018.
59. D. Jiang, Q. Yang, H. Wang, G. Zhu, J. Yang and C. Li, *J. Catal.*, 2006, **239**, 65-73.
60. D. Jiang, J. Gao, J. Yang, W. Su, Q. Yang and C. Li, *Micropor. Mesopor. Mater.*, 2007, **105**, 204-210.
61. J. Long, G. Liu, T. Cheng, H. Yao, Q. Qian, J. Zhuang, F. Gao and H. Li, *J. Catal.*, 2013, **298**, 41-50.
62. H. Zhang, R. Jin, H. Yao, S. Tang, J. Zhuang, G. Liu and H. Li, *Chem. Commun.*, 2012, **48**, 7874-7876.
63. F. Gao, R. Jin, D. Zhang, Q. Liang, Q. Ye and G. Liu, *Green Chem.*, 2013, **15**, 2208-2214.
64. R. Liu, R. Jin, L. Kong, J. Wang, C. Chen, T. Cheng and G. Liu, *Chem.–Asian J.*, 2013, **8**, 3108-3115.
65. X. Gao, R. Liu, D. Zhang, M. Wu, T. Cheng and G. Liu, *Chem.–Eur. J.*, 2014, **20**, 1515-1519.
66. R. Liu, R. Jin, J. An, Q. Zhao, T. Cheng and G. Liu, *Chem.–Asian J.*, 2014, **9**, 1388-1394.
67. Y. Xu, T. Cheng, J. Long, K. Liu, Q. Qian, F. Gao, G. Liu and H. Li, *Adv. Synth. Catal.*, 2012, **354**, 3250-3258.
68. D. Xia, T. Cheng, W. Xiao, K. Liu, Z. Wang, G. Liu, H. Li and W. Wang, *ChemCatChem*, 2013, **5**, 1784-1789.
69. Y. Shen, Q. Chen, L.-L. Lou, K. Yu, F. Ding and S. Liu, *Catal. Lett.*, 2010, **137**, 104-109.
70. B. Deng, T. Cheng, M. Wu, J. Wang and G. Liu, *ChemCatChem*, 2013, **5**, 2856-2860.
71. C. Chen, L. Kong, T. Cheng, R. Jin and G. Liu, *Chem. Commun.*, 2014, **50**, 10891-10893.
72. B. Deng, W. Xiao, C. Li, F. Zhou, X. Xia, T. Cheng and G. Liu, *J. Catal.*, 2014, **320**, 70-76.
73. P. Piaggio, C. Langham, P. McMorn, D. Bethell, P. C. Bulman-Page, F. E. Hancock, C. Sly and G. J. Hutchings, *J. Chem. Soc., Perkin Trans. 2*, 2000, 143-148.
74. P. Piaggio, P. McMorn, C. Langham, D. Bethell, P. C. Bulman-Page, F. E. Hancock and G. J. Hutchings, *New J. Chem.*, 1998, **22**, 1167-1169.
75. P. Piaggio, P. McMorn, D. Murphy, D. Bethell, P. C. Bulman Page, F. E. Hancock, C. Sly, O. J. Kerton and G. J. Hutchings, *J. Chem. Soc., Perkin Trans. 2*, 2000, 2008-2015.
76. H. Zhang, S. Xiang and C. Li, *Chem. Commun.*, 2005, 1209-1211.

77. H. Zhang, S. Xiang, J. Xiao and C. Li, *J. Mol. Catal. A: Chem.*, 2005, **238**, 175-184.
78. H. Zhang, Y. Zhang and C. Li, *J. Catal.*, 2006, **238**, 369-381.
79. H. Zhang and C. Li, *Tetrahedron*, 2006, **62**, 6640-6649.
80. P. Das, A. Silva, A. Carvalho, J. Pires and C. Freire, *Catal. Lett.*, 2009, **129**, 367-375.
81. L.-L. Lou, S. Jiang, K. Yu, Z. Gu, R. Ji, Y. Dong and S. Liu, *Micropor. Mesopor. Mater.*, 2011, **142**, 214-220.
82. G.-J. Kim and J.-H. Shin, *Tetrahedron Lett.*, 1999, **40**, 6827-6830.
83. K. Yu, L.-L. Lou, F. Ding, S. Wang, Z. Wang and S. Liu, *Catal. Commun.*, 2006, **7**, 170-172.
84. F. Bigi, L. Moroni, R. Maggi and G. Sartori, *Chem. Commun.*, 2002, 716-717.
85. D.-W. Park, S.-D. Choi, S.-J. Choi, C.-Y. Lee and G.-J. Kim, *Catal. Lett.*, 2002, **78**, 145-151.
86. R. I. Kureshy, I. Ahmad, N. H. Khan, S. H. R. Abdi, K. Pathak and R. V. Jasra, *Tetrahedron: Asymmetry*, 2005, **16**, 3562-3569.
87. R. I. Kureshy, I. Ahmad, N. H. Khan, S. H. R. Abdi, K. Pathak and R. V. Jasra, *J. Catal.*, 2006, **238**, 134-141.
88. K. Yu, Z. Gu, R. Ji, L.-L. Lou, F. Ding, C. Zhang and S. Liu, *J. Catal.*, 2007, **252**, 312-320.
89. H. Zhang, Y. M. Wang, L. Zhang, G. Gerritsen, H. C. L. Abbenhuis, R. A. van Santen and C. Li, *J. Catal.*, 2008, **256**, 226-236.
90. T. Roy, R. I. Kureshy, N. H. Khan, S. H. R. Abdi, A. Sadhukhan and H. C. Bajaj, *Tetrahedron*, 2012, **68**, 6314-6322.
91. A. R. Silva, K. Wilson, J. H. Clark and C. Freire, *Micropor. Mesopor. Mater.*, 2006, **91**, 128-138.
92. K. Yu, Z. Gu, R. Ji, L.-L. Lou and S. Liu, *Tetrahedron*, 2009, **65**, 305-311.
93. L.-L. Lou, K. Yu, F. Ding, X. Peng, M. Dong, C. Zhang and S. Liu, *J. Catal.*, 2007, **249**, 102-110.
94. J.-L. Zhang, Y.-L. Liu and C.-M. Che, *Chem. Commun.*, 2002, 2906-2907.
95. K. B. Sharpless, W. Amberg, M. Beller, H. Chen, J. Hartung, Y. Kawanami, D. Lubben, E. Manoury and Y. Ogino, *J. Org. Chem.*, 1991, **56**, 4585-4588.
96. I. Motorina and C. M. Crudden, *Org. Lett.*, 2001, **3**, 2325-2328.
97. H. M. Lee, S.-W. Kim, T. Hyeon and B. M. Kim, *Tetrahedron: Asymmetry*, 2001, **12**, 1537-1541.
98. D. Lee, J. Lee, H. Lee, S. Jin, T. Hyeon and B. M. Kim, *Adv. Synth. Catal.*, 2006, **348**, 41-46.
99. M. Iwamoto, Y. Tanaka, J. Hirosumi, N. Kita and S. Triwahyono, *Micropor. Mesopor. Mater.*, 2001, **48**, 271-277.
100. M. Iwamoto, Y. Tanaka, J. Hirosumi and N. Kita, *Chem. Lett.*, 2001, **30**, 226-227.
101. R. A. García, R. van Grieken, J. Iglesias, V. Morales and D. Gordillo, *Chem. Mater.*, 2008, **20**, 2964-2971.
102. S. Sahoo, P. Kumar, F. Lefebvre and S. B. Halligudi, *J. Catal.*, 2009, **262**, 111-118.
103. T. Ben Zid, I. Khedher and A. Ghorbel, *React. Kinet., Mech. Catal.*, 2010, **100**, 131-143.
104. S. Alavi, H. Hosseini-Monfared and P. Aleshkevych, *RSC Adv.*, 2014, **4**, 48827-48835.
105. R. A. Shiels, K. Venkatasubbaiah and C. W. Jones, *Adv. Synth. Catal.*, 2008, **350**, 2823-2834.
106. S. Sahoo, P. Kumar, F. Lefebvre and S. B. Halligudi, *Appl. Catal. A: Gen.*, 2009, **354**, 17-25.
107. G. Gerstberger and R. Anwander, *Micropor. Mesopor. Mater.*, 2001, **44–45**, 303-310.
108. J. K. Park, S.-W. Kim, T. Hyeon and B. M. Kim, *Tetrahedron: Asymmetry*, 2001, **12**, 2931-2935.
109. Y. Wan, P. McMorn, F. Hancock and G. Hutchings, *Catal. Lett.*, 2003, **91**, 145-148.
110. K. Pathak, A. P. Bhatt, S. H. R. Abdi, R. I. Kureshy, N.-u. H. Khan, I. Ahmad and R. V. Jasra, *Tetrahedron: Asymmetry*, 2006, **17**, 1506-1513.
111. K. Pathak, I. Ahmad, S. H. R. Abdi, R. I. Kureshy, N.-u. H. Khan and R. V. Jasra, *J. Mol. Catal. A: Chem.*, 2008, **280**, 106-114.
112. L. Zhang, Y. Guo, J. Peng, X. Liu, P. Yuan, Q. Yang and C. Li, *Chem. Commun.*, 2011, **47**, 4087-4089.
113. R. Jin, K. Liu, D. Xia, Q. Qian, G. Liu and H. Li, *Adv. Synth. Catal.*, 2012, **354**, 3265-3274.
114. K. Liu, R. Jin, T. Cheng, X. Xu, F. Gao, G. Liu and H. Li, *Chem.–Eur. J.*, 2012, **18**, 15546-15553.
115. A. Lee, W. Kim, J. Lee, T. Hyeon and B. M. Kim, *Tetrahedron: Asymmetry*, 2004, **15**, 2595-2598.
116. J.-M. Lee, J. Kim, Y. Shin, C.-E. Yeom, J. E. Lee, T. Hyeon and B. Moon Kim, *Tetrahedron: Asymmetry*, 2010, **21**, 285-291.
117. V. J. Mayani, S. H. R. Abdi, R. I. Kureshy, N.-u. H. Khan, A. Das and H. C. Bajaj, *J. Org. Chem.*, 2010, **75**, 6191-6195.
118. C. Baleizão, B. Gigante, H. Garcia and A. Corma, *J. Catal.*, 2003, **215**, 199-207.
119. J.-H. Kim and G.-J. Kim, *Catal. Lett.*, 2004, **92**, 123-130.
120. H. Yang, L. Zhang, P. Wang, Q. Yang and C. Li, *Green Chem.*, 2009, **11**, 257-264.
121. H. Yang, L. Zhang, W. Su, Q. Yang and C. Li, *J. Catal.*, 2007, **248**, 204-212.
122. Y.-S. Kim, X.-F. Guo and G.-J. Kim, *Chem. Commun.*, 2009, 4296-4298.
123. A. Corma, H. Garcia, A. Moussaif, M. J. Sabater, R. Zniber and A. Redouane, *Chem. Commun.*, 2002, 1058-1059.
124. A. R. Silva, V. Guimaraes, A. P. Carvalho and J. Pires, *Catal. Sci. Technol.*, 2013, **3**, 659-672.
125. C. S. Gill, K. Venkatasubbaiah and C. W. Jones, *Adv. Synth. Catal.*, 2009, **351**, 1344-1354.
126. E. Gross, J. H. Liu, S. Alayoglu, M. A. Marcus, S. C. Fakra, F. D. Toste and G. A. Somorjai, *J. Am. Chem. Soc.*, 2013, **135**, 3881-3886.
127. T. T. Adint and C. R. Landis, *J. Am. Chem. Soc.*, 2014, **136**, 7943-7953.

Transition–metal–functionalized ordered mesoporous silicas: An overview of sustainable chiral catalysts for enantioselective transformations

Tanyu Cheng, Qiankun Zhao, Dacheng Zhang, and Guohua Liu*

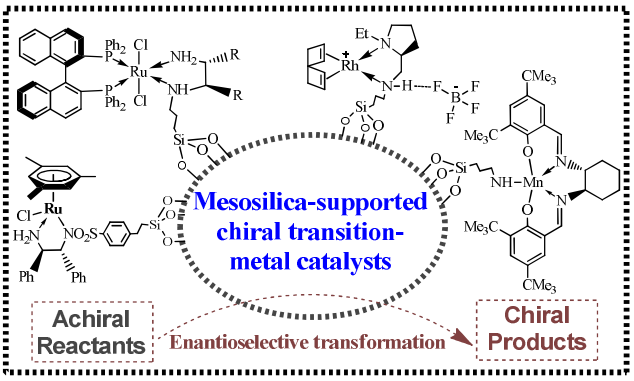

This review focuses on the development of ordered mesoporous silica-supported chiral transition-metal-based catalysts for enantioselective transformations.